3-2-3 Data processing

The following map shows a flow chart of data analysis.

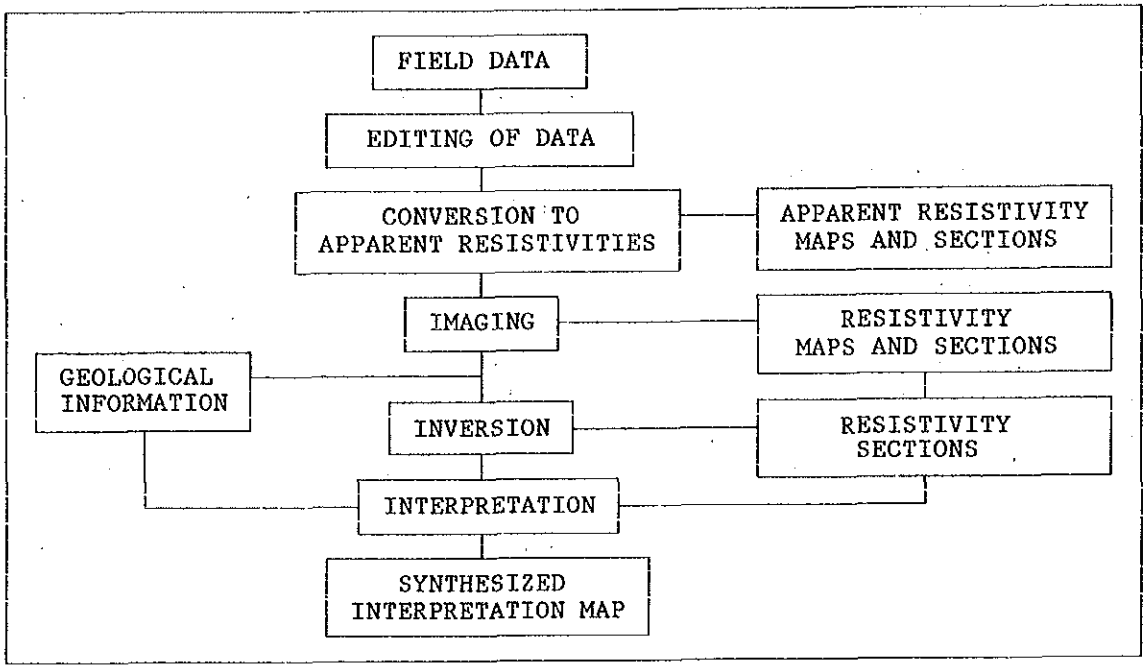

In the first phase of data processing, the decay voltages are transformed into late-time apparent resistivity values at each gates, after checking the measurement parameters (e.g., loop dimensions, gains of receiver, current, location and so forth) of field data.

The voltages(in unit of mV) which are measured by the PROTEM57(C) system are converted to magnetic field decay rate, dB/dt(Nv/m^2), by the following formula.

$$dB/dt=V*192/(2^{n}*RXA/100) \quad (1)$$

where RXA is the receiver coil moment(m^2), and n is the front panel gain setting. Apparent resistivities ρa(ohm-m) are then given by,

$$\rho a=[\mu/(4\pi t)]*[0.4*\mu*TXM/(t*dB/dt)]^{2/3} \quad (2)$$

where μ is magnetic permeability($4\pi*10^{-7}$ in unit of H/m), t is measurement time in ms, and TXM is transmitter moment which is the product of loop area(m^2) and current(A).

A rapid inversion technique called "imaging" has recently been developed for estimating resistivity as a function of depth from TEM sounding data (Fullagar, 1989; Eaton and Hohmann, 1989). Using this technique, we can transform response measured as a function of time into resistivity values as a function of depth. Imaging solutions are not

restrained by artificial parameterization of the Earth into a finite number of layers or biased by the choice of initial models which are required by model-fitting routines.

Therefore, in this survey, we obtained resistivity structures with continuous function of depth for all the survey profiles by imaging technique.

A program named "IMAGE II", developed by the University of Utah, was used to produce imaging resistivity structures. The imaging technique is based on the same principle employed by Fullagar(1989); resistivities are computed directly from time-derivative data, dB/dt, and then associated with a depth to calculate an estimated resistivity. The resistivity is the conventional apparent resistivity, ρa, and the assigned depth is the depth to the physical current maximum at the delay time in question for a half-space of resistivity ρa. This approach is close to that proposed by Raiche and Gallagher(1985). They, however, used the depth of maximum |dB/dt| as their measure of penetration depth, while Fullagar(1989) used the depth at which |E|(current) is maximum. The penetration depth, Dp, can be expressed as a function of time,

$$D_p(t) = \int_0^t V_d[\rho_a(t'), t']\, dt'. \qquad (3)$$

where $\rho a(t')$ is apparent resistivity at gate time t' and Vd is the vertical diffusion velocity of the physical current maximum.

The 1-D inverse processing is used to obtain one-dimensional resistivity structures for some profiles where can be assumed to be the layered model from geological point of view. In this process, a candidate model is iteratively changed and computed curves are fitted to the observed data by the least squares method. The boundaries of one dimensional models along a survey line may then be connected to allow comparison of inversion data with geological cross sections.

The program, which was used is "TEMIXGL" of Interpex Ltd., can estimate structural parameters (e.g., resistivities and thickness) of best fitting models with up to 8 layers using automatic ridge regression. In these calculations, imaging results were used to estimate initial model parameters.

2-D forward modeling was also carried out to clarify the resistivity structure in the region with a two dimensional inhomogeneous resistivity structure. This method is based on the classical DuFort-Frankel finite-difference scheme, which is both explicit and stabile for any size of time step(Oristaglio and Hohmann, 1984). The program which we have used in this study is "TDEM2D" which was developed by the University of Utah.

3-3 Survey results

3-3-1 TEM survey

The survey points were located by open traverse method on grid with a N-S spacing of 100 m and an E-W spacing of 200 m, as shown in Fig.II-3-1. The survey grid was oriented relative to magnetic north.

"Central loop" TEM soundings were made at almost all of the stations (see figure). In these soundings, the transient magnetic field was measured by a multiturn receiver located at the center of the transmitter loop. The transmitter loop dimensions were 100 m x 100 m and the current was about 12 A.

Around Tsagaan Tolgoi, in the central part of the survey area, the "Turam" sounding mode was utilized for detailed surveying. This mode employs a large fixed transmitter loop and a small roving receiver to make measurements along lines perpendicular to the loop. For the Turam measurements, a transmitter loop 100m x 200 m with its long axis oriented E-W, was used (Fig.II-3-2). At 6 stations in an area of rugged limestone outcrop in the northwestern part of the survey area, the Turam soundings were made with a loop 100m x 100 m.

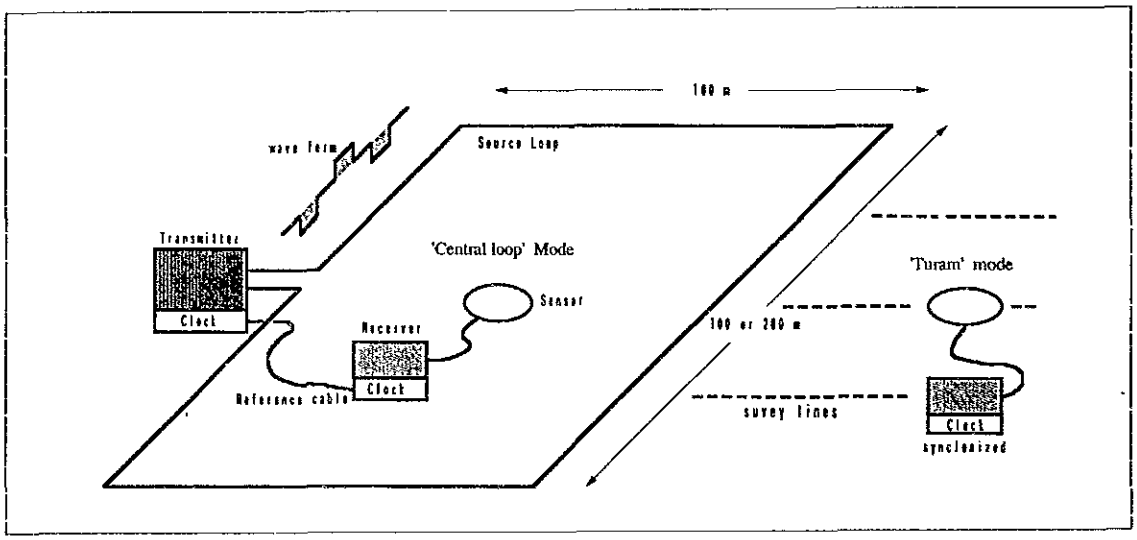

Measurements were made at a total of 548 stations. These points were numbered relative to a Cartesian coordinate system whose origin was at the southwestern end of the survey area. The station numbers are four digit integers. The first two are the X (E-W) coordinate of the station and the last two digits are the Y (N-S) coordinates. Both coordinates are in hundreds of meters. For example, station 1814 is located 1,800 m west and 1,400 m north of the origin.

A transmitter current of about 9.0 A was driven through the 100 x 200 m loop and the current ranged from 11.0 to 12.5 A through the 100 x 100 m loop. There was little electromagnetic noise in the majority of the survey

area and 256 or 512 stacks were sufficient. Near the drilling site in Tsagaan Tolgoi the noise generated by the drill rig was appreciable and measurements were made when the rig was inoperative.

Data recorded at station 1616 exhibited a magnetic field polarity reversal. This was caused by drillhole casing inside the source loop and the data was ignored as being unusable.

Whenever data obtained was found to vary drastically from data recorded at near by stations, additional measurements were made to reduce uncertainties.

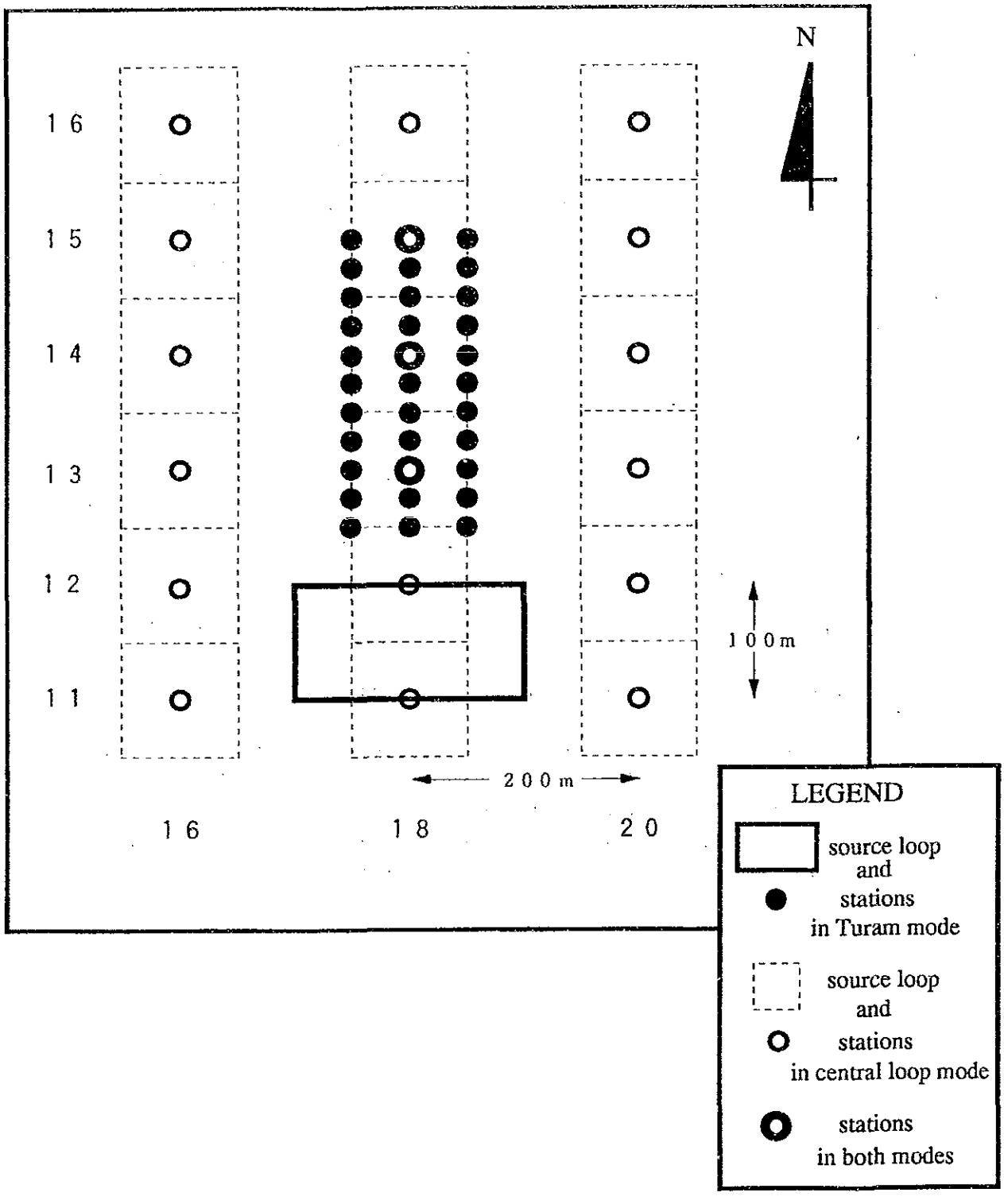

Fig. II-3-2 TEM survey configurations at Tsagaan-Tolgoi

3-3-2 Laboratory resistivity measurement of rock samples

Forty-three rock samples were collected during the course of the survey at sites shown in Fig.II-3-1. Cubic samples 3 cm large were cut from these rocks for resistivity measurements. The resistivity samples were soaked in fresh water for 24 hours and naturally dried before the resistivity measurements were made. The densities and FE's (induced polarization frequency effect) were also measured during testing. The results of these measurements are given in Tab.II-3-1 and may be summarized as follows.

1) The resistivities of samples range from 258 to 44,200 ohm-m.
2) Quartz samples show resistivities of 18,000 ohm-m or more, although some of the veins in the Tsagaan Tolgoi contain ore. The resistivity of sandstone which surrounds these veins is around 3,000 ohm-m, or 6 to 7 times more conductive.
3) Limestone and shale samples had average resistivities in excess of 5,000 ohm-m.
4) The resistivity of the diorite which is distributed in the southwestern and southeastern parts of the survey area was about 3,000 ohm-m. Altered diorite which was collected around the fault and near quartz veins is much more conductive (250 to 1,200 ohm-m).
5) Dacite from the northern part of the survey area (390 to 1,910 ohm-m) is 4 to 10 times more conductive than the surrounding shale and sandstone.
6) The FE values of all of the samples were found to be low, ranging from 0.0 to 0.6 %.
7) The altered andesite and diorite samples were found to be the densest with densities of 2.8 g/cc or more. Dacite samples were found to have the lowest densities (2.46 g/cc) and other samples were found to range in density from 2.6 to 2.7 g/cc. The density contrast of the majority of the samples was found to be less than 0.2 g/cc.

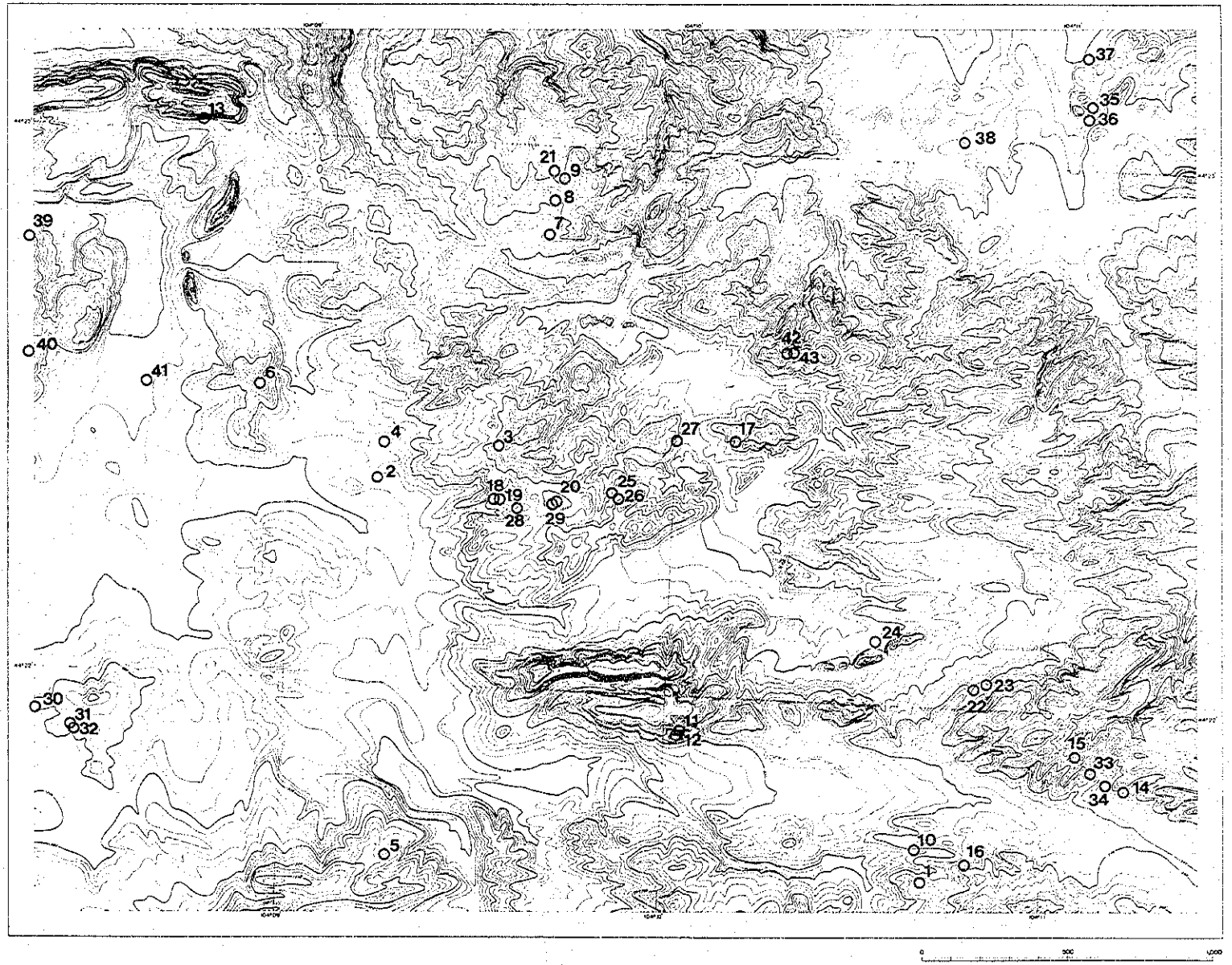

LEGEND

○15 Sampling Point

Fig. II-3-3 Rock samples location map

Tab.II-3-1 Rock Properties

NO	ROCKNAME	RESISTIVITY (ohm-m)		DENSITY (g/cc)		FE (%)	COMMENT
		MEAN	AVE	MEAN	AVE		
1		3,420		2.68		0.4	
2		4,190		2.66		0.4	with Qtz vein
3		1,410		2.62		0.3	fine, core
4		2,720		2.67		0.4	
5	sandstone	4,390	2,974	2.66	2.67	0.4	silicified
6		5,470		2.71		0.5	greenish gray
7		1,650		2.70		0.4	greenish gray
8		2,160		2.65		0.4	greenish gray
9		3,870		2.67		0.5	greenish gray
10		6,550		2.72		0.3	
11		10,500		2.69		0.4	
12	limestone	20,200	7,903	2.76	2.72	0.4	
13		10,600		2.65		0.5	
14		7,040		2.83		0.5	
15		2,350		2.66		0.4	
16		15,100		2.66		0.4	
17		6,170		2.61		0.4	
18	quartz	20,200	18,774	2.64	2.63	0.4	
19		15,300		2.60		0.4	
20		44,200		2.63		0.3	
21		34,400		2.64		0.5	
22	altered	2,350	4,480	2.83	2.84	0.3	
23	andesite	8,540		2.85		0.3	
24		658		2.71		0.2	
25	altered	348		2.69		0.2	
26	diorite	488	511	2.74	2.71	0.4	
27		258		2.78		0.0	
28		1,210		2.62		0.4	pyrhytization
29		1,410		2.78		0.3	boring core
30		6,760		2.90		0.5	micro
31	diorite	13,800	5,168	2.93	2.88	0.5	micro
32		11,300		2.95		0.5	
33		1,780		2.84		0.5	micro
34		7,200		2.86		0.4	micro
35		390		2.32		0.2	
36	dacite	903	707	2.56	2.46	0.4	
37		1,910		2.62		0.4	
38		514		2.35		0.2	
39		3,640		2.70		0.4	greenish gray
40		15,300	8,719	2.76	2.71	0.5	silicified
41	shale	11,900		2.68		0.6	silicified, fg
42		2,510	5,950	2.68	2.69	0.4	black shale
43		14,100		2.69		0.6	black shale
	AVERAGE		3,880		2.69	0.4	

3-3-3 Apparent resistivity

The decay voltages which are measured by the PROTEM receiver are transformed into late-time apparent resistivity values at each gates using equation (2) as mentioned in "Data Processing". In this section, these results are presented as plots of late-time apparent resistivity versus time for visual inspection and graphical interpretation (maps: PL.II-3-2, 3, and 4, sections: PL.II-3-5, 6, and 7). Pseudo-apparent resistivity maps of gates 2, 6, and 12 at a base frequency of 30 Hz are shown in Fig.II-3-4, 5, and 6. The corresponding decay voltages were recorded at 0.108, 0.278, and 1.06 ms after the current was turned off. Assuming an average resistivity of 100 ohm-m, these times correspond to depth of 70, 120, and 230 m, respectively.

Pseudo-apparent resistivity sections of NS-line 02, 18, and 34 are shown in Fig.II-3-7, 8, and 9, respectively.

Apparent resistivity map (t=0.108 ms, Fig.II-3-4)

Wide spread relatively resistive areas (200 ohm-m or more) can be seen in the northwestern, southern, and east-central parts of the survey area. These generally correspond to limestone, shale, and schist outcrops. In the south-central survey area, there is a zone trending NE-SW along a fault with a resistivity of less than 100 ohm-m. There is also a parallel high resistivity zone (150 ohm-m) or more north of this fault. In the northern part of the survey area, a low resistivity area with 50-100 ohm-m can be seen and there is an area with resistivities of less than 50 ohm-m in the northeastern part of the survey area.

Apparent resistivity map (t=0.278 ms, Fig.II-3-5)

The general features of this map are consistent with the previous map(Fig.II-3-4). There is a clear low resistivity area in the northeast with a small zone of less than 10 ohm-m, which indicates that a low resistivity zone should exist at a depth of more than 100 m.

Apparent resistivity map (t=1.06 ms, Fig.II-3-6)

The resistive areas of this map, related to limestone, shale, or schist occurrence, are generally unchanged from the previous two maps. It is worth noting that the conductive zone, which was seen along the fault at earlier times, however, has become relatively resistive (100 to 150 ohm-m).

Apparent resistivity "pseudo-sections" for all NS lines are presented in PL.II-3-5 to 7. Fig.II-3-7(a), (b), and (c) are apparent resistivity pseudo-sections for NS lines 02, 18, and 34, respectively. These figures are pseudo-sections in that they show the apparent resistivity of the earth beneath the measurement station as a function of time rather that depth.

The measurement time is shown on the vertical axis at the right end of the section and the corresponding gate channel is given on the left vertical axis. The horizontal axis is the grid coordinate and the station number is shown above the section. The first two digits of the station numbers, which are the line number, have been deleted in these figures.

For instance, station 1814 is shown as "14" on the section for NS line-18.

Apparent resistivity section (NS line-02, Fig.II-3-7(a))

This profile is resistive (>200 ohm-m) north of station 20 with a shallow conductor beneath station 30. South of station 20, the top of the section is generally conductive, but a resistive electrical basement is seen after gate 15. There is a local resistivity low from station 14 through 18 which may be related to a wadi seen at station 18. The resistive zone (>200 ohm-m) from station 06 through 09 continues to the northeast.

Apparent resistivity section (NS line-18, Fig.II-3-7(b))

The section is conductive (50 to 100 ohm-m) north of station 20, resistive from station 20 through 15 and resistive south of station 02. Between stations 14 and 02 a resistive basement, seen after gate 17, is overlain by a conductive unit.

The resistive area of 150 ohm-m or more in center of the profile corresponds to the resistive zone which trends NE-SW in apparent resistivity maps. A quartz veins outcrops near Tsagaan Tolgoi (station 14) , but no anomalous resistivity values are seen. The more conductive zone, of 100 ohm-m or less, between
stations 10 and 12 is situated near a fault.

Apparent resistivity section (NS line-34, Fig.II-3-7(c))

This section is conductive north of station 21, where there is a known fault, and resistive to the south with a high contrast of resistivities from north to south. In the south, values are generally over 300 ohm-m with marginally more conductive values at very early times. Resistivities at the northern end of the profile are beneath 75 ohm-m and decrease with time.

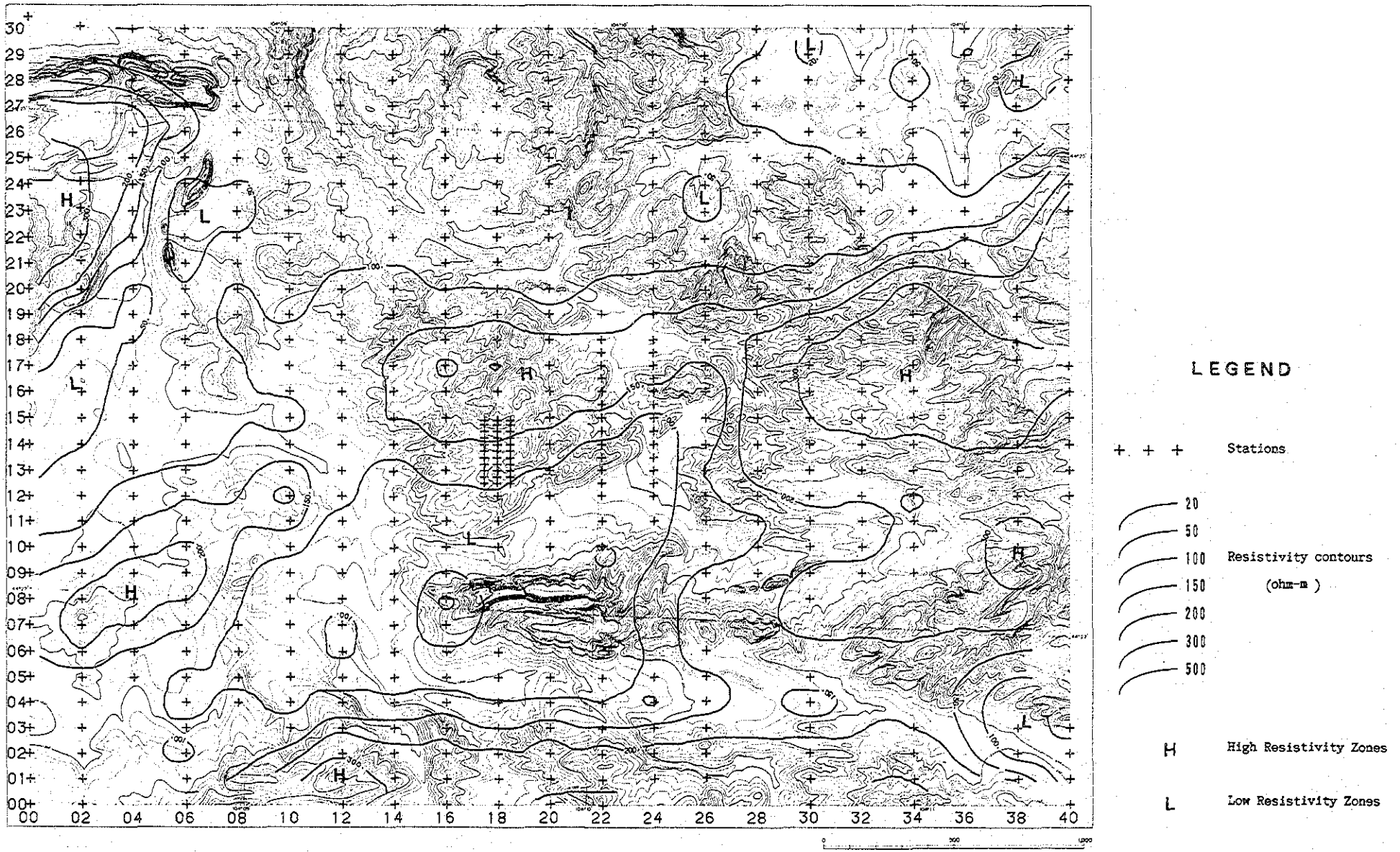

Fig. II-3-4 Apparent resistivity pseudo-map (t=0. 108msec)

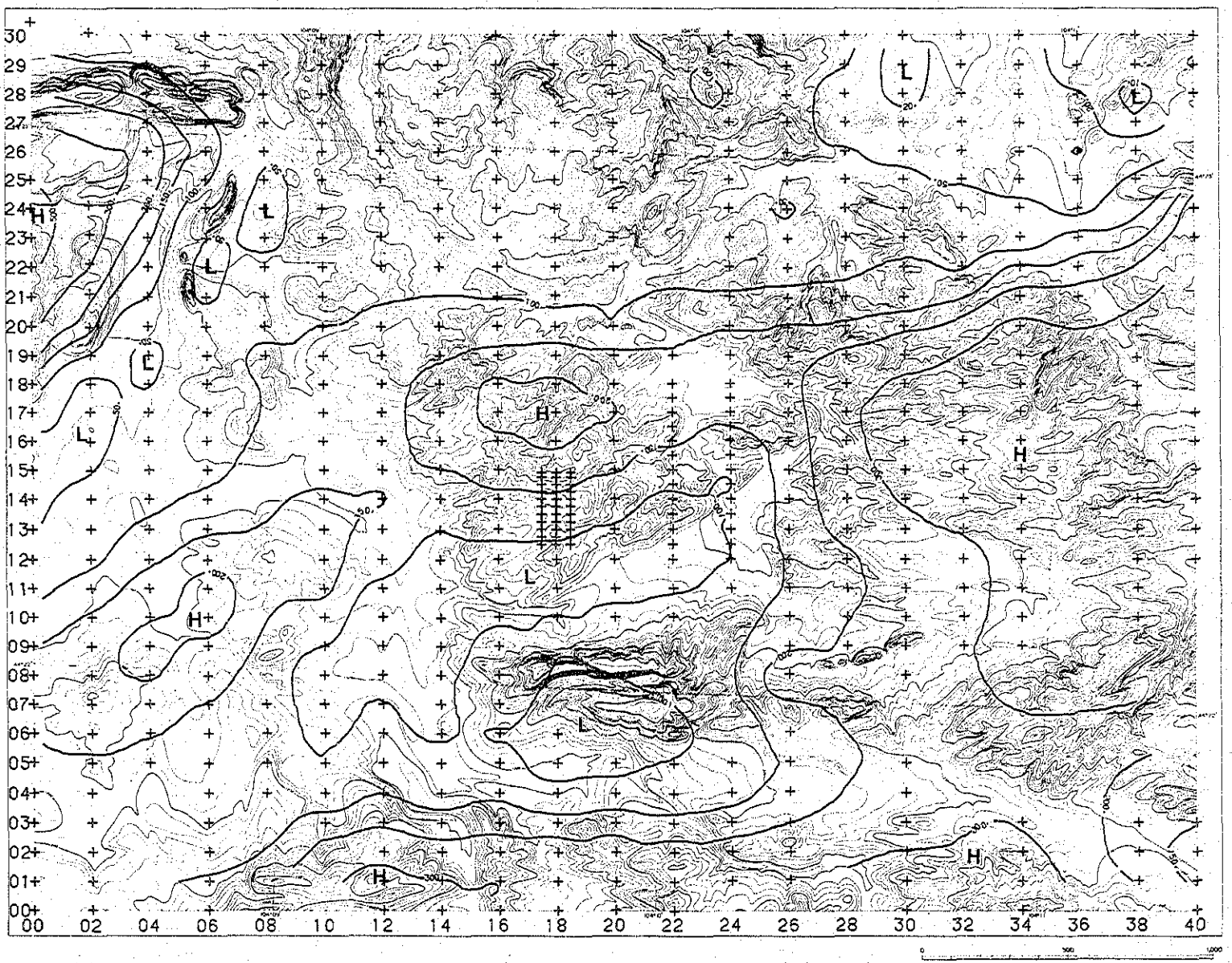

Fig. II-3-5 Apparent resistivity pseudo-map (t=0.278msec)

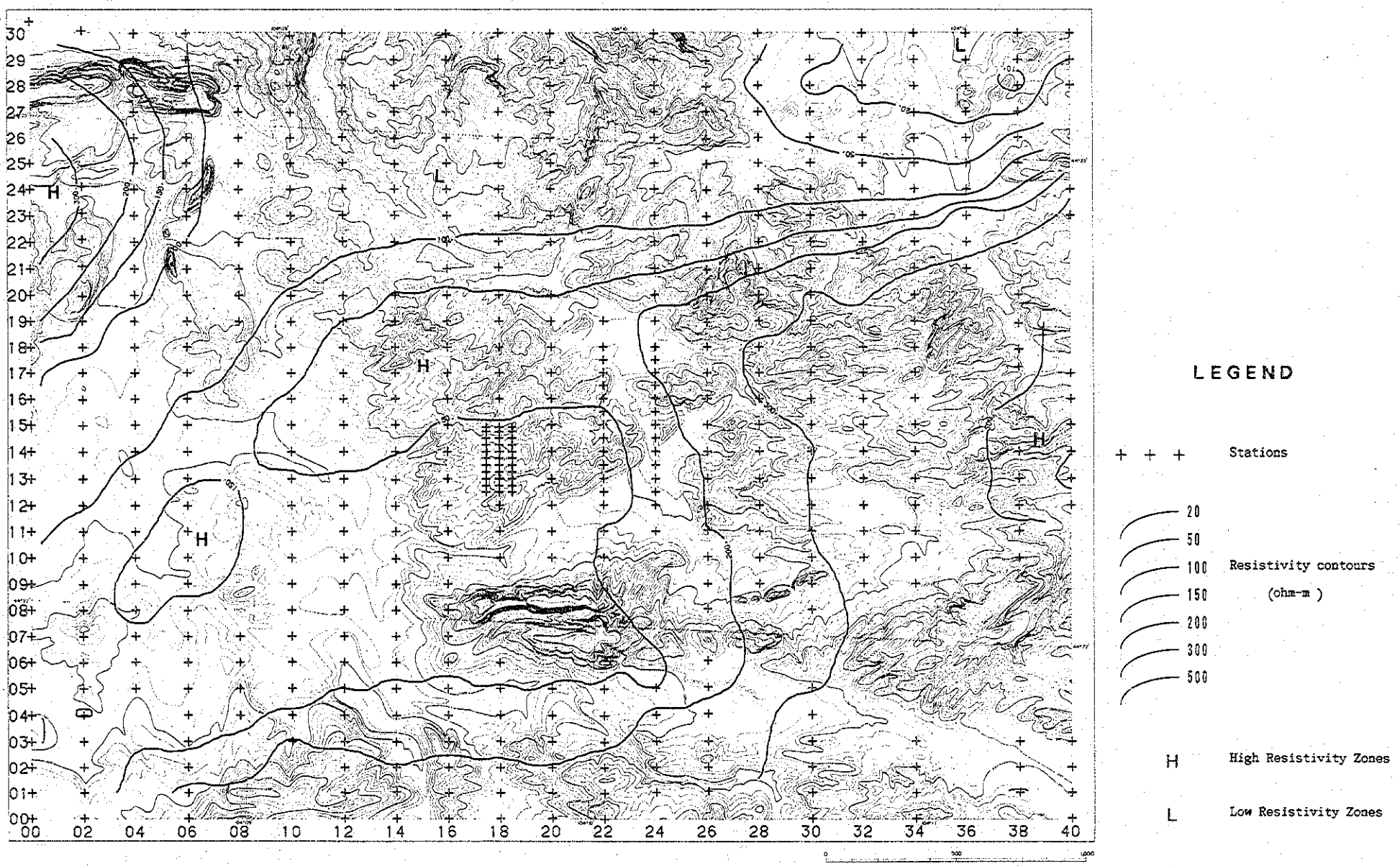

Fig. II-3-6 Apparent resistivity pseudo-map (t=1.06msec)

(a)

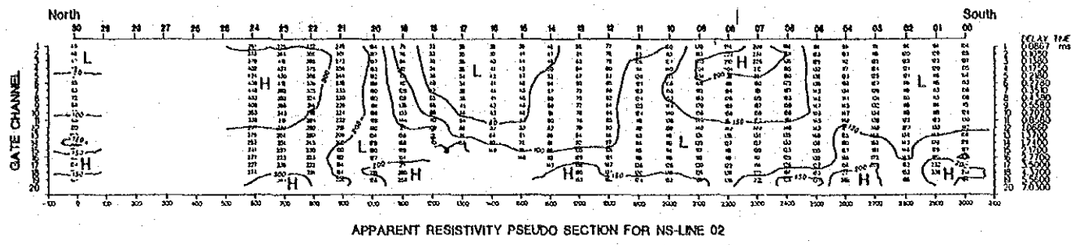

APPARENT RESISTIVITY PSEUDO SECTION FOR NS-LINE 02

(b)

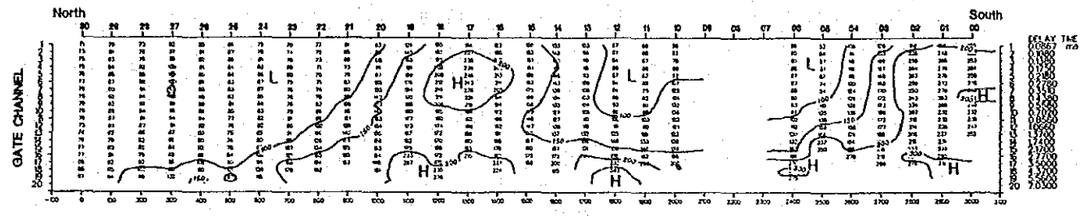

APPARENT RESISTIVITY PSEUDO SECTION FOR NS-LINE 18

(c)

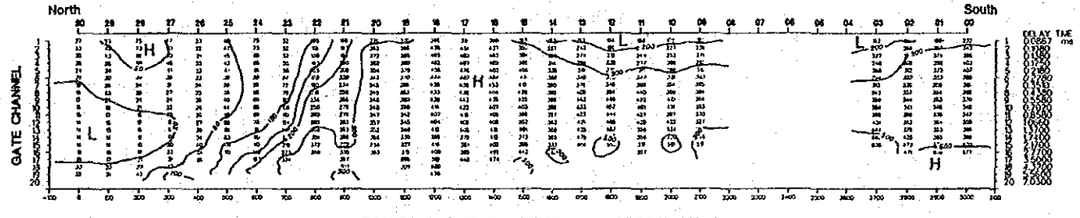

APPARENT RESISTIVITY PSEUDO SECTION FOR NS-LINE 34

LEGEND

15 ..... Station Number

..... Topography

20
50
100 Resistivity Contours
150
200 (Ω・m)
300
500

H High Resistivity Zone

L Low Resistivity Zone

Fig. II-3-7 Apparent resistivity pseudo-sections for NS lines 02, 18 and 34

3-3-4 Resistivity structures

1) Imaging

Comparison of imaging and 1-D inversion results (Fig.II-3-8)

Imaging and one dimensional (1-D) inversion results were compared, to check the efficiency of image processing of the data collected in this survey. Image processing was found to be suitable and the data was converted to resistivity structures by the imaging method.

Imaging and 1-D results, for NS line 18, are presented for comparison in Fig.II-3-8. The structural features revealed by imaging in resistive area generally resemble the 1-D inversion results. In central part of the profile, conductive layer 3 detected by 1-D inversion, appears to be a tabular conductor which outcrops near stations 11 and 12 and dips to the north. While one of the advantages of the imaging technique is high resolution of conductive units, this layer was not detected by image inversion in the northern part of the profile. This is probably due to the lower resistivity contrast between layers 2 and 3 in the north than in the central part of the profile. We, furthermore, conclude that interpretation of the results from 1-D inversion in laterally heterogeneous areas should be carried out with caution. Imaging, however, produces resistivity structures which are similar to spacially filtered 1-D inversion results.

Contoured resistivity image maps of the survey area at levels of 1,150, 1,100, 1,050, and 1,000 m above sea level (ASL) are presented in PL.II-3-8 to 11 and Fig.II-3-9 to 12.

Resistivity image map (1,150 m level, Fig.II-3-9)

This map shows the resistivity distribution at a depth of around 50 m. In the southern and eastern parts of the survey area, which are predominatly limestone, green schist, and sandstone, there is high resistivity zone (>200 ohm-m). In the center of the area, there is a zone of low resistivity (<100 ohm-m) which trends NE-SW. This zone occures along the Olon Ovoot fault which is a major fault in this area. North of the fault, a zone with resistivity of 150 ohm-m or more strikes approximately parallel to the fault. The dense resistivity contour lines between the resistive eastern and the conductive northeastern areas strike NE-SW, along the Olon Ovoot fault.

The northern part of the survey area has a relatively constant resistivity of 50-100 ohm-m. To the east of this zone, there ia a flat plane with a resistivity of 50 ohm-m or less. The main conductive zone, which extends to the north of the survey area, is estimated to have a resistivity of less than 10 ohm-m.

A low resistivity zone of 50 ohm-m or less 200 m wide strikes NE-SW in the northwestern survey area. While the southern part of this conductive zone is situated nearly along the "wadi", the northern part is more than 400 m the wadi.

Resistivity image map (1,100 m level, Fig.II-3-10)

Fig.II-3-10 resembles the map of the 1,150 m level. The resistive zone north of and parallel to the Olon Ovoot fault is clearer, in spite of slightly lower resistivities.

The constant reisistivity zone with 100 ohm-m or less in the northern part of the survey area is more widespread than in the previous map(Fig.II-3-9) and it includes green schist and sandstone areas.

The conductive zone in the northeast has an E-W width of 600 m or more. The northwestern survey area which is predominately limestone has a resistivity of 150-200 ohm-m.

Resistivity image map (1,050 m level, Fig.II-3-11)

The zone along the Olon Ovoot fault which was conductive in the previous maps(Fig.II-3-9 and 10) has become resistive with 200 ohm-m or more. North of the fault, the high resistivity zone parallel to the fault has become indistinct.

The limestone, green schist, and sandstone areas are unchanged with a resistivities of 250 ohm-m or more.

The conductive zone in the northeastern survey area has developed more complex branch-like features which are extensions of the resistive zone.

Resistivity image map (1,000 m level, Fig.II-3-12)

While the majority of the area is resistive at this depth, there is a zone with a resistivity of 200 ohm-m or less in the northern part of survey area which trends E-W.

The central part of survey area has resistivities of 300 ohm-m or more along the Olon Ovoot fault.

Area with resistivities of 500 ohm-m or more are seen only in the limestone zone in the eastern survey area and have decrease in size as the depth has increased. The resistivity contrast has generally decreased from the previous maps.

Resistivity image sections for all NS profiles are presented in PL.II-3-13 to 15. The sections for NS lines 02, 18, 24, and 34 are shown in Fig.II-3-13. Three sections around Tsagaan Tolgoi in central part of the survey area are shown in Fig.II-3-14.

Resistivity image section (NS line-02, Fig.II-3-13(a))

There is a broad zone of 20-50 ohm-m in the center of this section. The conductive zone between stations 15 and 18 is situated around a wadi.

North of the conductive zone (from stations 21 to 24), resistivities of 200 ohm-m or more are estimated to extend to depths of 500 m more.

Resistivities above 200 ohm-m at depths of 100 m from station 07 to 09 in the southern part of the profile may imply an area of shale and andesite rocks. This resistive zone continues to the NE(Fig.II-3-9).

Resistivity image section (NS line-18, Fig.II-3-13(b))

This section crosses the quartz vein which outcrops in the Tsagaan Tolgoi area near station 14. A major resistive zone is detected from station 15 through 18 in this section a few hundred meters north of the outcrops at station 14 near Tsagaan Tolgoi. The surface layer around stations 11 and 12, near the Olon Ovoot fault, is conductive with a resistivity of 50-100 ohm-m. This conductive zone dips to the north or the northwest in this section and in NS lines 16 to 24(PL.II-3-13).

Near the fault, the section is resistive at depths of 150 m or more, and conductive at depths less than 100 m, as seen in the image maps. The low resistivity zone near surface at station 05 may be due to groundwater beneath the wadi.

While the green schist area in the northern part of section is homogeneous with resistivities of 50-100 ohm-m, the structures in the southern end of the profile are complex with resistivities ranging from 80 to 1,000 ohm-m. There is a layer of 200 ohm-m or less dipping to the south at an angle of about 45 degrees to the horizontal at the southern end of this section.

Resistivity image section (NS line-24, Fig.II-3-13(c))

This section crosses the Olon Ovoot fault near station 14 at an angle of approximately 45 degrees. The surface layer near the fault (stations 12 to 14) has resistivities of 100 ohm-m or less. There is also a low resistivity zone dipping to the north and a resistive zone under the conductive area along the fault in this section, as in NS line-18.

The northern part of this profile, where pelitic schist are distributed, shows uniform resistivities of 50-100 ohm-m, similar to NS line-18. There is a local conductive zone near surface around statios 23 and 24. This conductor is also seen in section 26(PL.II-3-13).

A layer with resistivity of around 200 ohm-m dips to the south in sandstone and shale in the southern part of the section.

Resistivity image section (NS line-34, Fig.II-3-13(d))

The resistivity structures varies dramatically around stations 23 and 24 in this section. High resistivities, which extends to depths of 400 m or more, are seen in the green schist and limestone areas in the southern part of the section and very conductive zone (<50 ohm-m) is seen beneath the flat plane at the northern end of the section. There is also a remarkable flat-lying conductor (<20 ohm-m) beneath stations 27 through 30. The conductor extends to the north and is also seen in NS lines 28 to 40, PL.II-3-13 and 14.

Resistivity image sections (Tsagaan Tolgoi, Fig.II-3-14(a),(b),(c))

Three sections, paralleled to NS line-18 around Tsagaan Tolgoi, are shown in this figure. There is a vertical resistive body, with a width of 70 m, beneath stations 13 and 14 in each of the profiles. This resistive

vein-like body is more distinct on the west side of the sections. It has a resistivity of 100-150 ohm-m and dips to the north.

There is no anomalous structure around station 14, where a quartz vein outcrop striking E-W can be seen.

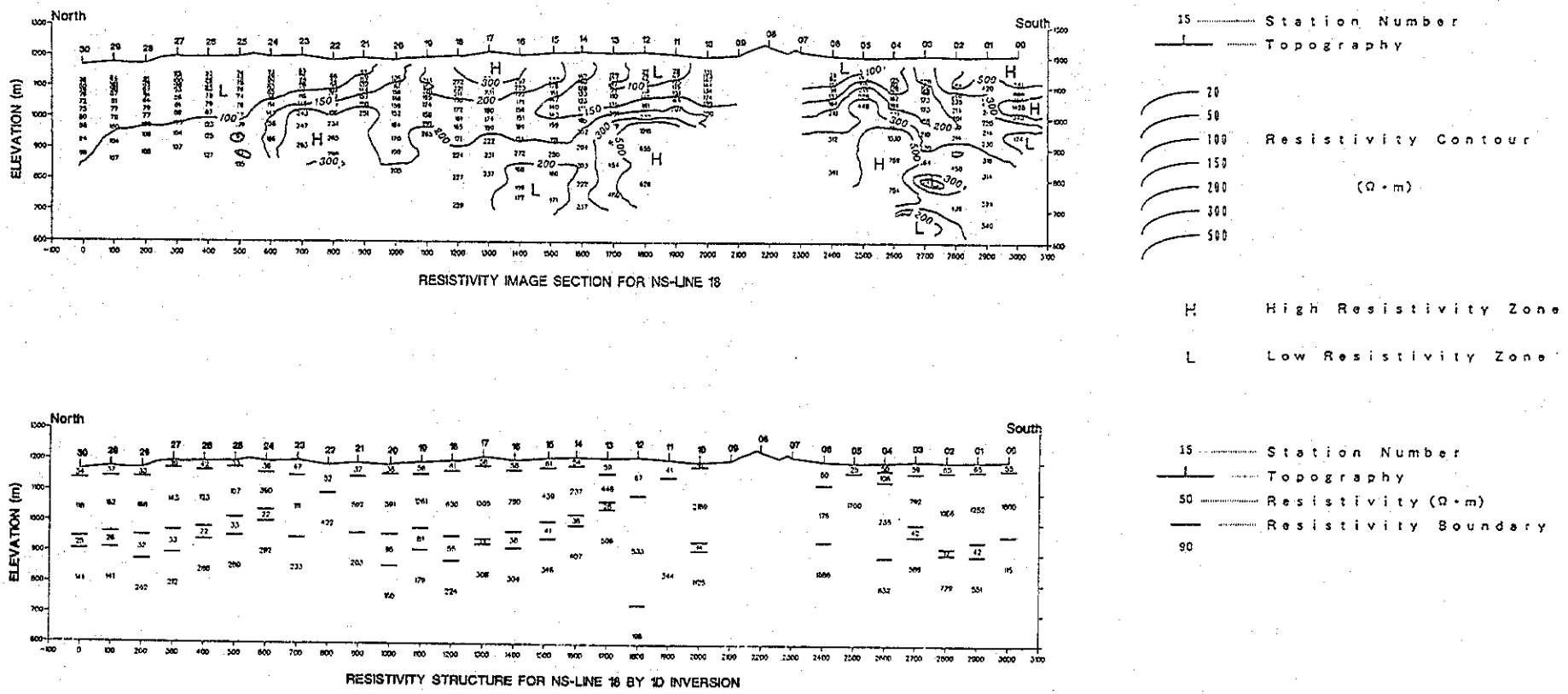

Fig. II-3-8 Comparison of imaging and inversion results for NS line 18

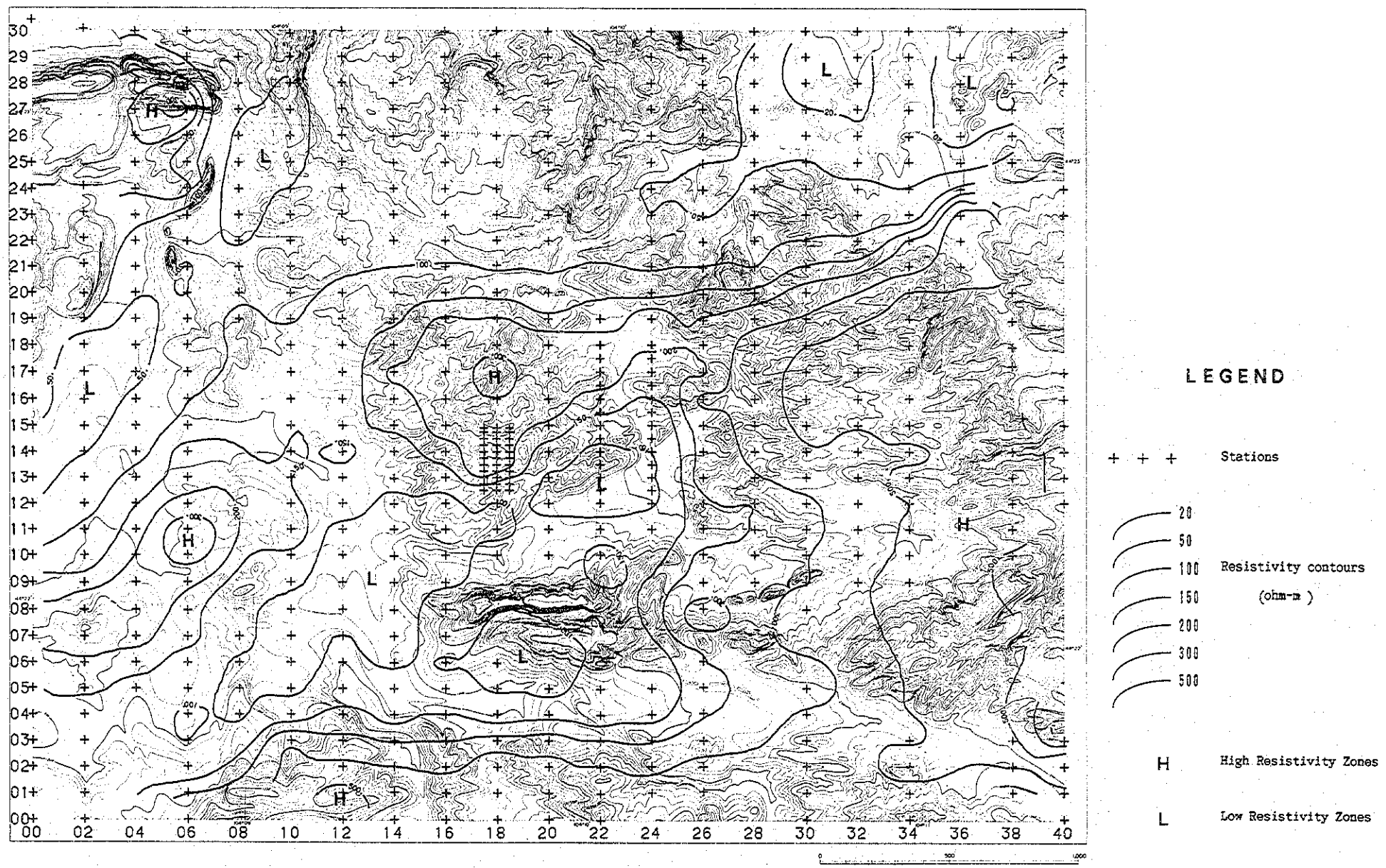

Fig. II-3-9 Resistivity image at the 1150m level

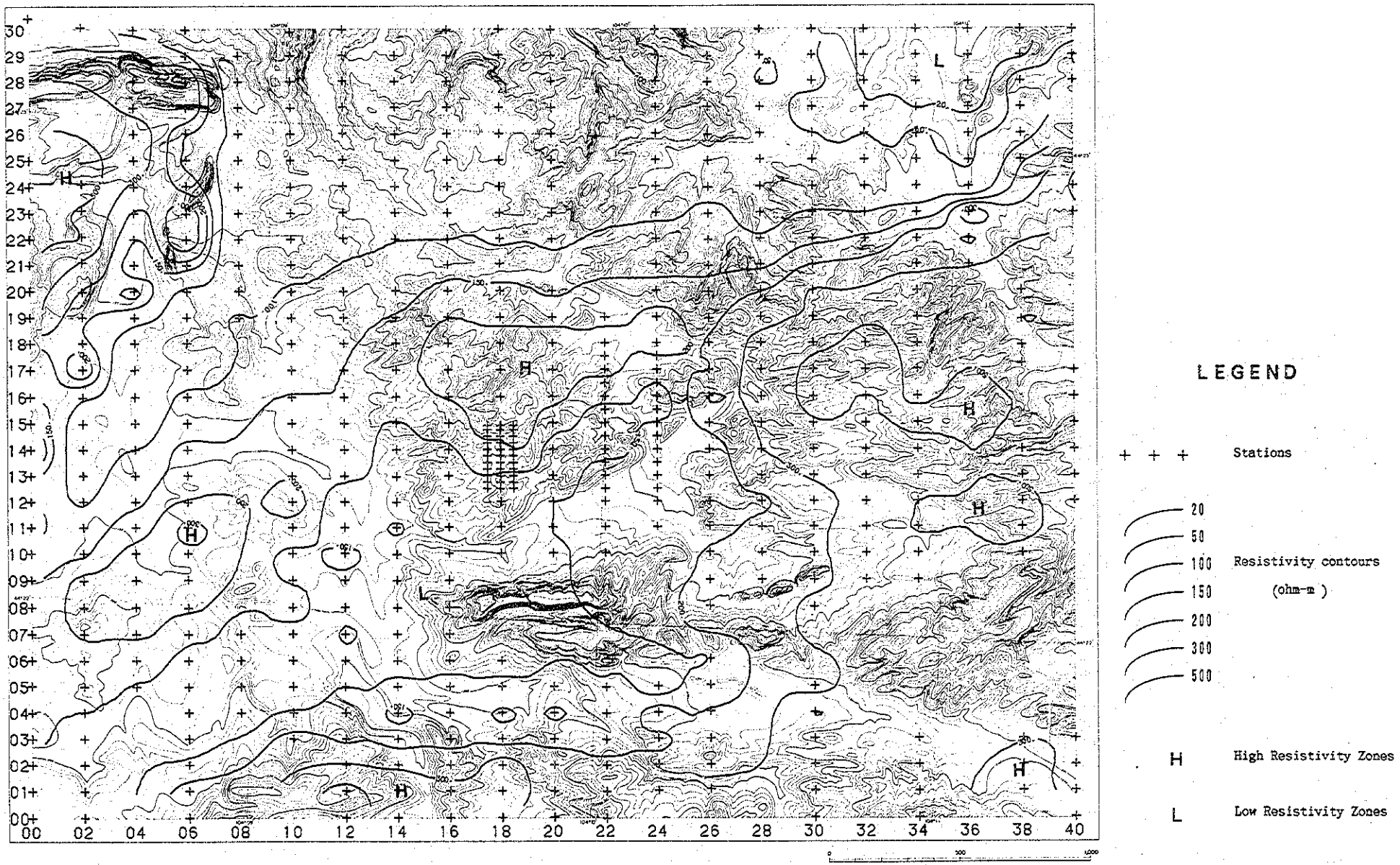

Fig. II-3-10 Resistivity image at the 1100m level

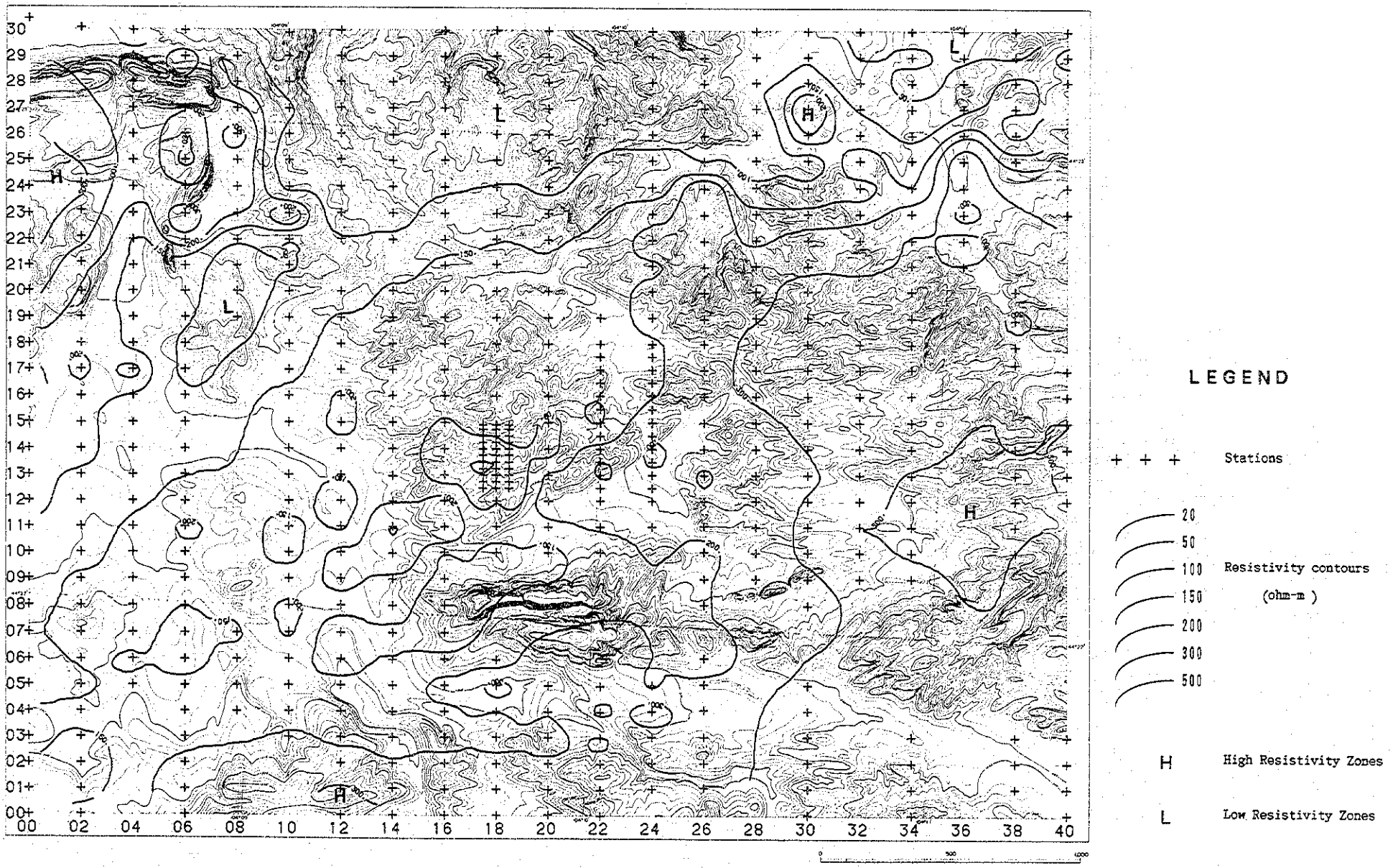

Fig. II-3-11 Resistivity image at the 1050m level

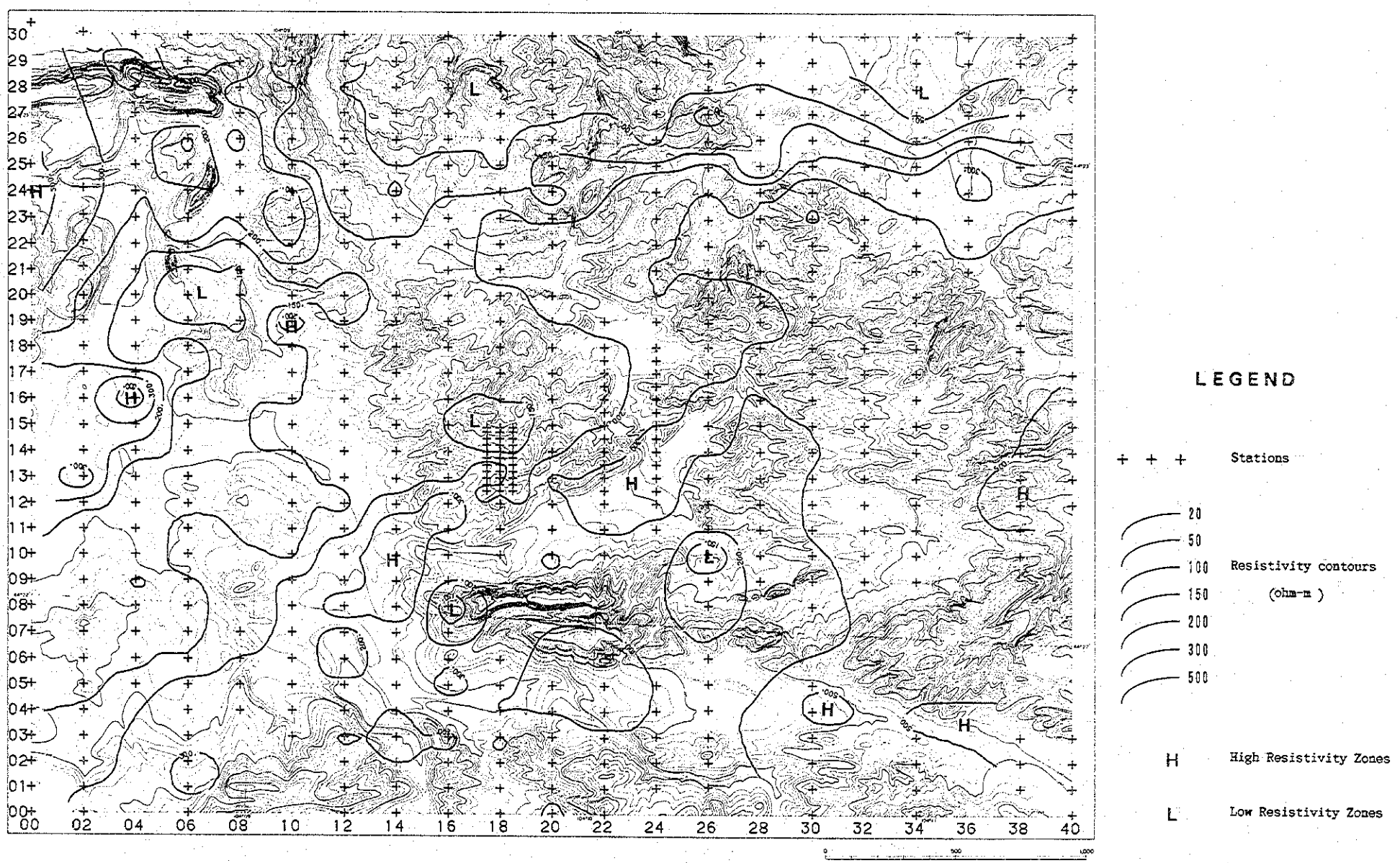

Fig. II-3-12 Resistivity image at the 1000m level

(a)

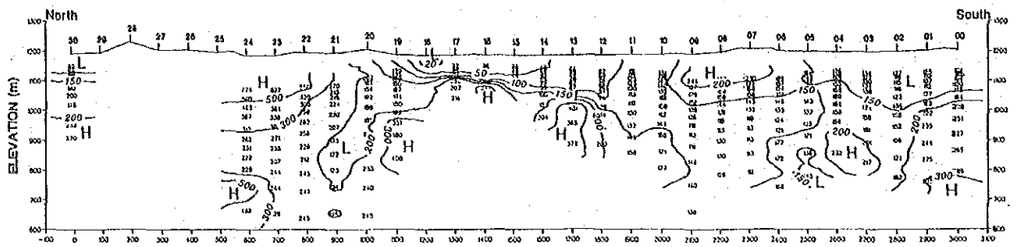

RESISTIVITY IMAGE SECTION FOR NS-LINE 02

(b)

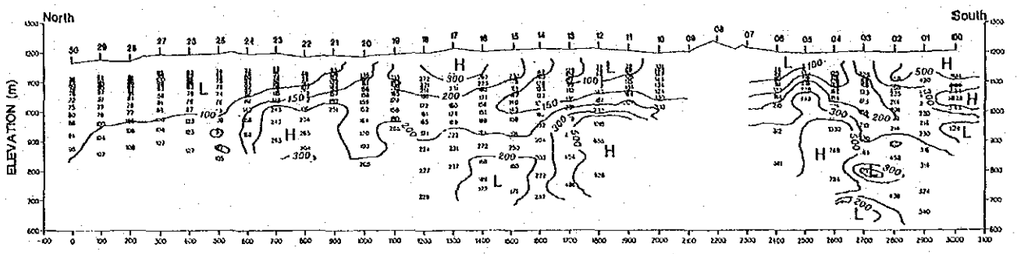

RESISTIVITY IMAGE SECTION FOR NS-LINE 18

(c)

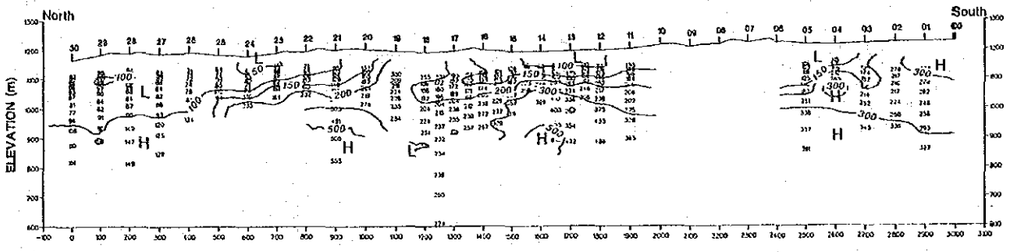

RESISTIVITY IMAGE SECTION FOR NS-LINE 24

(d)

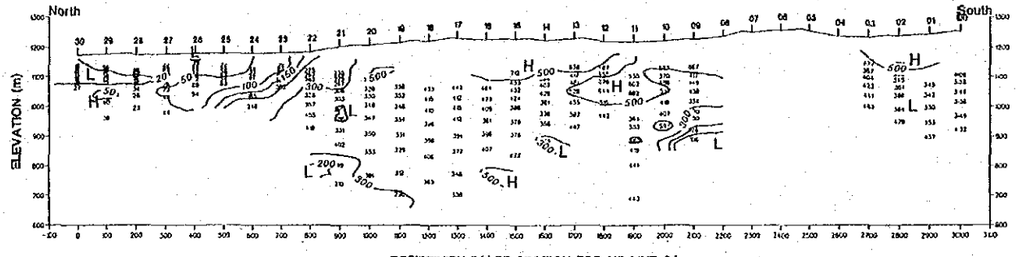

RESISTIVITY IMAGE SECTION FOR NS-LINE 34

LEGEND

15 ..... Station Number

..... Topography

20
50
100 Resistivity Contours
150
200 (Ω·m)
300
500

H High Resistivity Zone

L Low Resistivity Zone

Fig. II-3-13 Resistivity image sections for NS lines 02, 18, 24, and 34

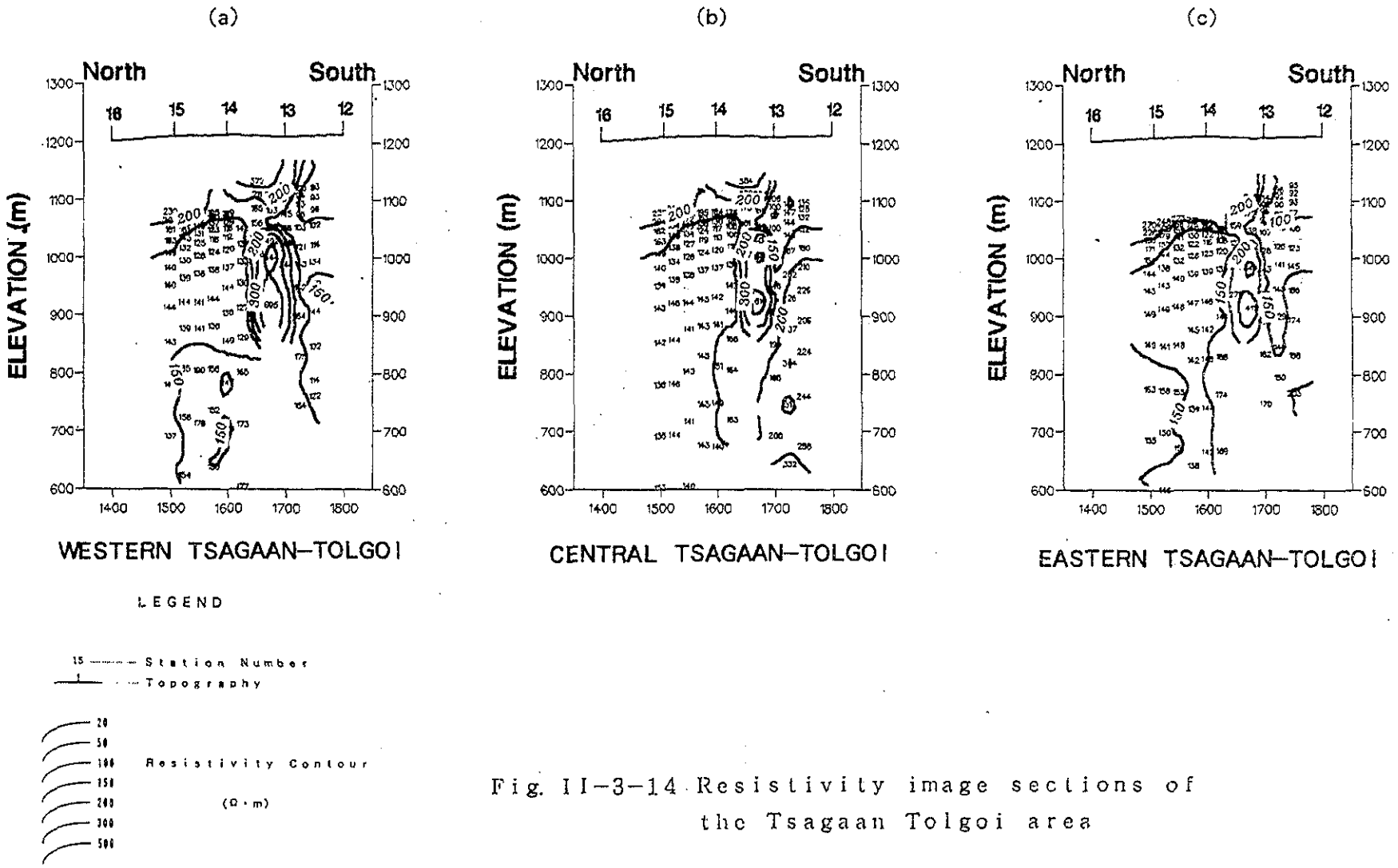

Fig. II–3–14 Resistivity image sections of the Tsagaan Tolgoi area

2) 1-D inversion results

1-D inversions were carried out to clarify quantitative features of some interesting profiles wich showed only weak three dimensional effects. These inversions were performed by a nonlinear least squares procedure and imaging results were used in determination of candidate models.

The northeast of survey area

Fig.II-3-15 shows the resistivity profiles from the northeastern part of the survey area. A major conductive body, with a resistivity of less than 10 ohm-m, was detected along NS lines 30 to 38. It has a thickness of 10-100 m at the depth of 50-90 m. This conductor is near surface at the east and west ends of these profiles and is more than 50 m deep in the center of the sections.

The resistivity of the basement beneath the conductive layer is less than 100 ohm-m and it might be sandstone which occures primarily in the northern part of the survey area. The conductive layer is bounded to the south by limestone and green schist. This zone seems to generally correspond an area which is predominately dacite. However, the conductive layer (<10 ohm-m) is not always seen in the dacite outcrops as seen stations 3029, 3030, 3629, and elsewhere in Fig.II-3-15.

The Olon Ovoot fault

Fig.II-3-16(a) and (b) show the resistivity structures across the Olon Ovoot fault along NS lines 22 and 24, respectively. We conducted a detailed survey along these lines with a spacing of 50 m near the fault.

In Fig.II-3-16(a) there is a shallow conductive layer of 20-90 ohm-m near the fault underlain at a depth of 50 to 140 m by a resistive layer of more than 400 ohm-m. The resistivity contrasts between this resistive layer and the surrounding basement is approximately in excess of 1.6.

The Olon Ovoot fault is near station 2414 in Fig.II-3-16(b). The resistivity structure of this section is similar to that of NS line-22. There is a subsurface low resistivity layer of 20-50 ohm-m near the fault and a high resistivity basement of greater than 400 ohm-m at the depth of 20-100 m. The resistivity contrast to the outer basement layer is more than 1.4.

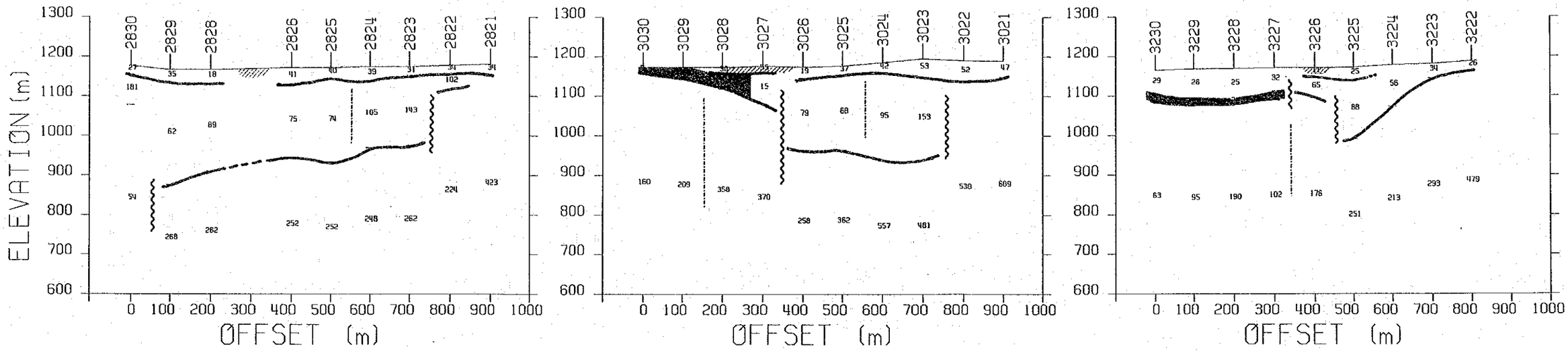

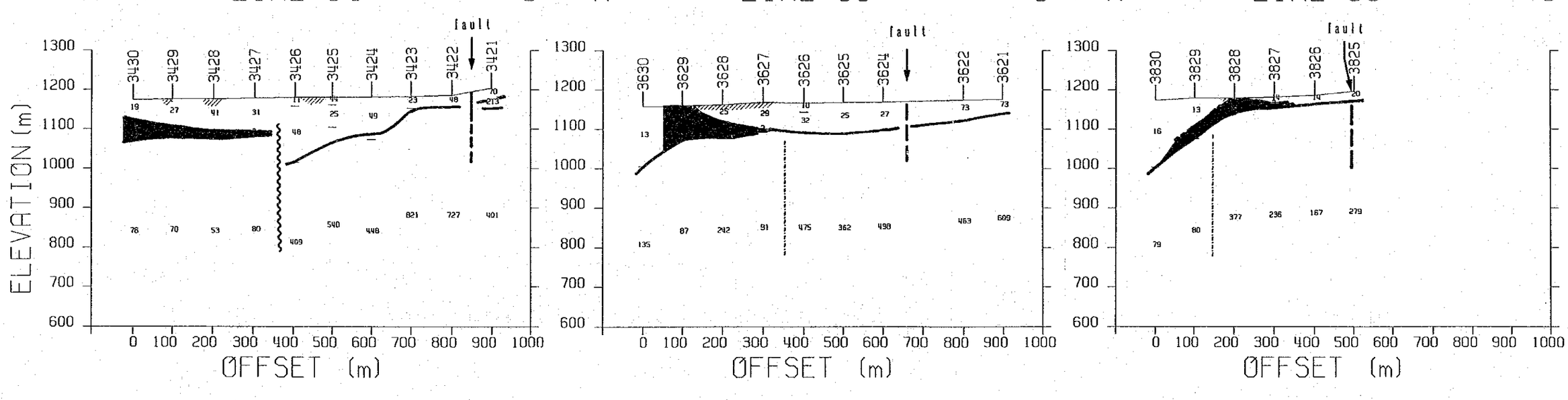

conductive zone (≦10ohm-m)

dacite outcrops

Fig. II-3-15 Resistivity sections of the northeastern survey area

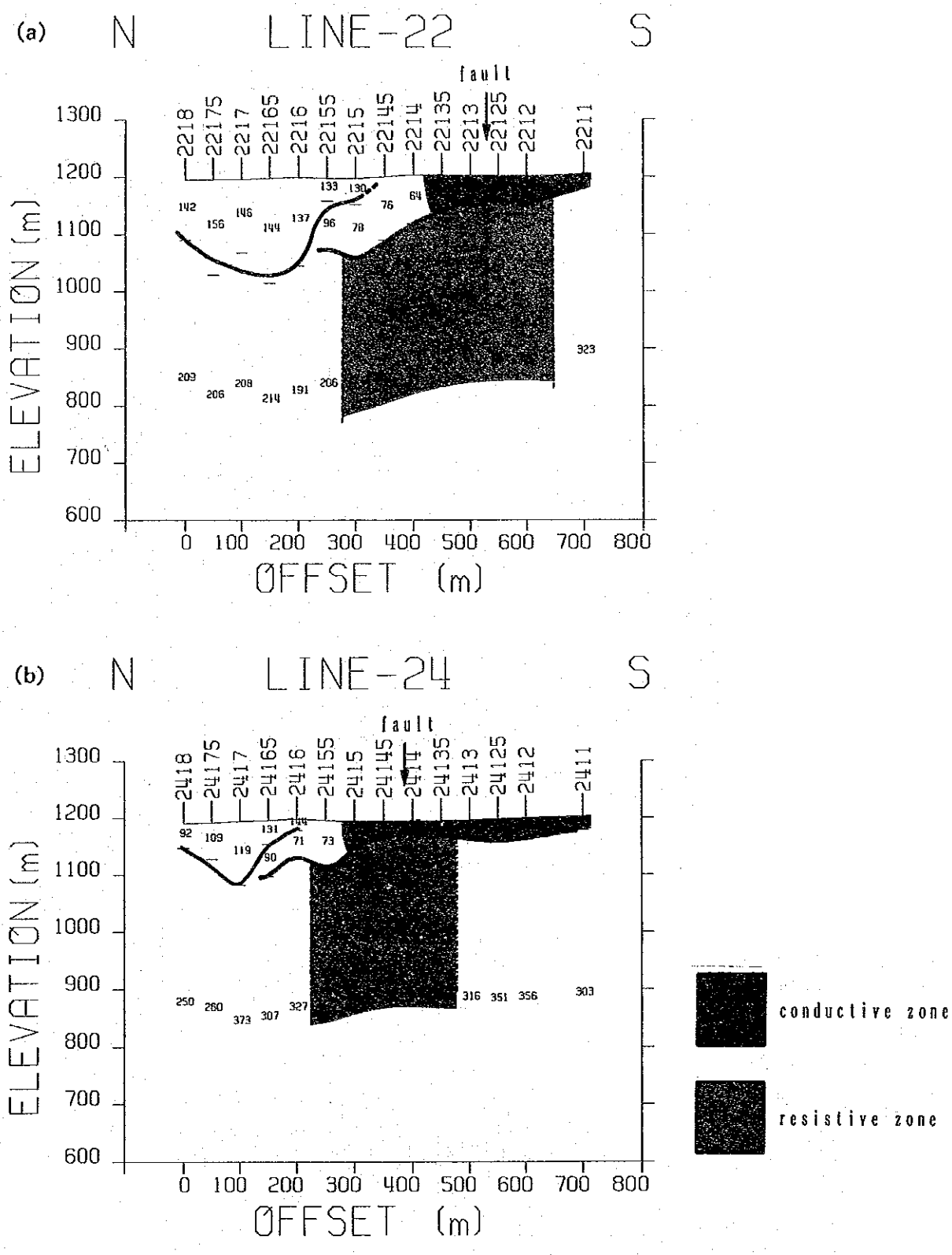

Fig. II-3-16 Resistivity sections of NS lines 22 and 24 around the Olon Ovoot fault

3) 2-D modeling results

The 2-D forward modeling have been performed to confirm the existence of the resistive body which was detected by imaging of detailed Turam data collected near Tsagaan Tolgoi.

The 2-D resistivity model, which were derived from the imaging results are shown as Model A in Fig.II-3-17(a). Model-A contains a vein-like resistive body which has a width of 75 m, a vertical thickness of 270 m and a resistivity of 1,000 ohm-m. Fig.II-3-17(b) shows Model B without vein-like resistive body. A resistor in both models is beneath station 1814 at Tsagaan Tolgoi, where a quartz vein is known to outcrop.

Data which was collected at stations 1814 and 181325 are shown in Fig.II-3-17(c) and (d), respectively. These curves represent the response for gates one through eight, normalized with respect to maximum positive response. Positive values are shown by solid lines and the negative values are shown by dashed lines. A reversal in the polarity of the response is seen at early time at station 1814. This is characteristic of data collected in the Turam configuration when the sensor is outside of the source loop. The results of 2-D forward calculations for models A and B are also shown in these figures by circles and triangles, respectively.

The theoretical response of 2-D model A fit the data from station 181325 with a lower average error than that produced by model B (Fig.II-3-17(c)). There is, however, a substantial misfit a very early times which implies that the shallow part of the section is more conductive (<175 ohm-m) in this area. Model-A also produces more satisfactory results than model B at station 1814 (Fig.II-3-17(d)).

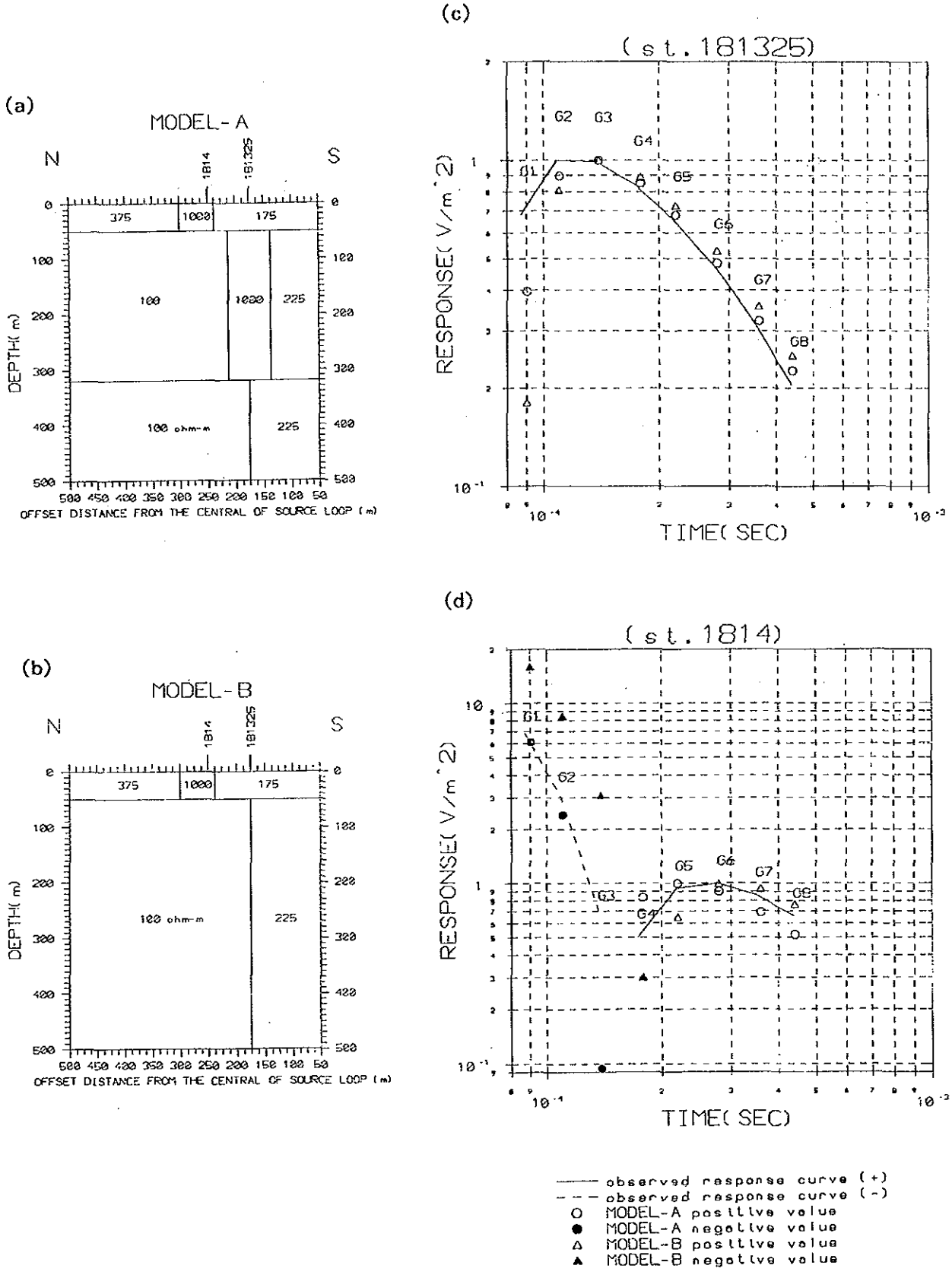

Fig. 11-3-17 2D-modeling of the Tsagaan Tolgoi area

3-4 Discussions and conclusions

Earth resistivity models which agree with the known geology have been derived from the TEM survey data by imaging and 1-D inversion. We shall discuss the following items;

Imaging and 1-D inversion

It was found that resistivity structures could be derived from imaging without bias or artificial parameterization of the Earth into a finite number of layers. 1-D inversion was carried out, however, for more quantitative interpretation of the TEM data. In this survey, only data from the northeastern part of survey area and around the Olon Ovoot fault was analyzed by 1-D inversion. The rest of the data was converted to resistivities as a function of depth by imaging. When imaging results were used to estimate initial inversion models, a good fit to the data could be obtained quickly.

Tsagaan Tolgoi area

The central part of the Olon Ovoot ore deposit area is situated in transition zone between a horizontal low resistivity extension along the Olon Ovoot fault and a high resistivity zone parallel to the fault (Fig.II-3-18). This resistive zone may represent the Silurian sandstone area rather than the quartz veins. The quartz vein outcrops of Tsagaan Tolgoi have not shown high resistive values.

There are two possible causes for these results. The first is that the accuracy of PROTEM57(C) is limited at shallow depths and in the survey the minimum depth of investigation was 50 to 100 m. Solution for depth shallower than this limit are not possible due to interference from the trasmitter shutoff ramp at early times. Therefore, this indicates that the quartz vein outcrops at Tsagaan Tolgoi does not exist to the adequate depth.

The second possibility is equivalence of resistive quartz veins and conductive disseminated ore zones. A detailed Turam survey was carried out along three profiles at Tsagaan Tolgoi. In this survey, the vertically tabular resistor 70 m wide, striking E-W, was detected around station 181325(25 meters north of station 1813) as illustrated in Fig.II-3-14. The resistive body is more distinct on west side of these three sections. Also according to the 2-D forward modeling, the calculated voltages from the model contained vein-like 1,000 ohm-m resistive body and observed data compare favorably with each other. Thus the body is thought be rocks contained quartz vein.

The Olon Ovoot fault

A low resistivity zone of 50 to 100 ohm-m was detected along the Olon Ovoot fault as shown in 1,150 m and 1,100 m level resistivity maps (Fig.II-3-9 and 10). Beneath this conductive zone a resistive zone (>400 ohm-m) is seen (Fig.II-3-16) along the fault near station 2413. It is surrounded by

a more conductive layer (200 to 300 ohm-m) and is greater than 400 m wide. An alteration zone, which was detected by geological survey, is shown north of the fault in the central part of the survey area. These facts can be stated that the subsurface conductive zone and the underlying resistive zone along the Olon Ovoot fault represent hydrothermal alteration and silicified zone, respectively. On the other hand, in a water well located near station 1005 the depth to groundwater is 2 m. This well is in a low resistivity zone in the southwestern part of the survey area along the fault at a low elevation, where the is topography is flat. Consequently, the southwestern part of the subsurface conductive zone along the fault is probably related to groundwater.

The northeast of survey area

In the northeastern part of the survey area, from NS profile 32 to 36, there is major conductive layer of 10 ohm-m or less. This layer is a excess of 500 m NS and 1,000 m EW and extends into the north of survey area(Fig.II-3-11). Resistivity values derived from 1-D inversion are less than 5 ohm-m in the central part of the conductive zone. The thickness of the layer ranges from 10 to 50 m and it is deep in the central area and shallow at the edges of the area. This area is predominatly Jurassic volcanic rocks, basalt and dacite, and is coincident with magnetic anomalies which were detected during topographic surveying. Laboratory measurements showed dacite rock samples to have the lowest resistivities(Table.II-3-1). Dacite outcrops, however, seem to be distributed in areas where a layer of 20-50 ohm-m covers the more conductive layer. One reasonable explanation for the low resistivities and magnetic anomalies could be the presence of a sulfide deposit.

Local subsurface conductive zone near station 2624 seems to be a fault striking NE-SW.

The western survey area

A zone of low resistivity (<50 ohm-m) 200 m wide, striking NE-SW, was detected in the northwestern survey area. A fault may be inferred along this zone, but none was detected during the geological survey.

As our main conclusion, we believe the following resistivity anpmalies may possibly be related to ore deposition, Fig.II-3-17. These resistivity anomalies are;

1) the vein-like resistive anomaly at Tsagaan Tolgoi(around station 1813),
2) the conductive anomaly in the northeastern part of the survey area(from NS line 32 to 36), and
3) the shallow conductive and deep resistive anomaly along the Olon Ovoot fault near station 2413.

In this study, we conducted TEM survey in order to map alteration zones and geological structure. This mapping has detected some resistivity anomalies which may be related to ore deposition. The results presented in this report show the potential of using TEM sounding method for exploration in rock desert areas such as this.

In the next stage of this survey, further investigation(e.g., three component TEM) will be required to determine the detailed resistivity structure in Olon Ovoot and along the Olon Ovoot fault. It is difficult to assess the geological validity of the inversion results in the northeastern survey area, where a major conductive zone was detected, due to the sparse station density. In order to check the relationship between this low resistivity zone and ore deposition, drilling is recommended.

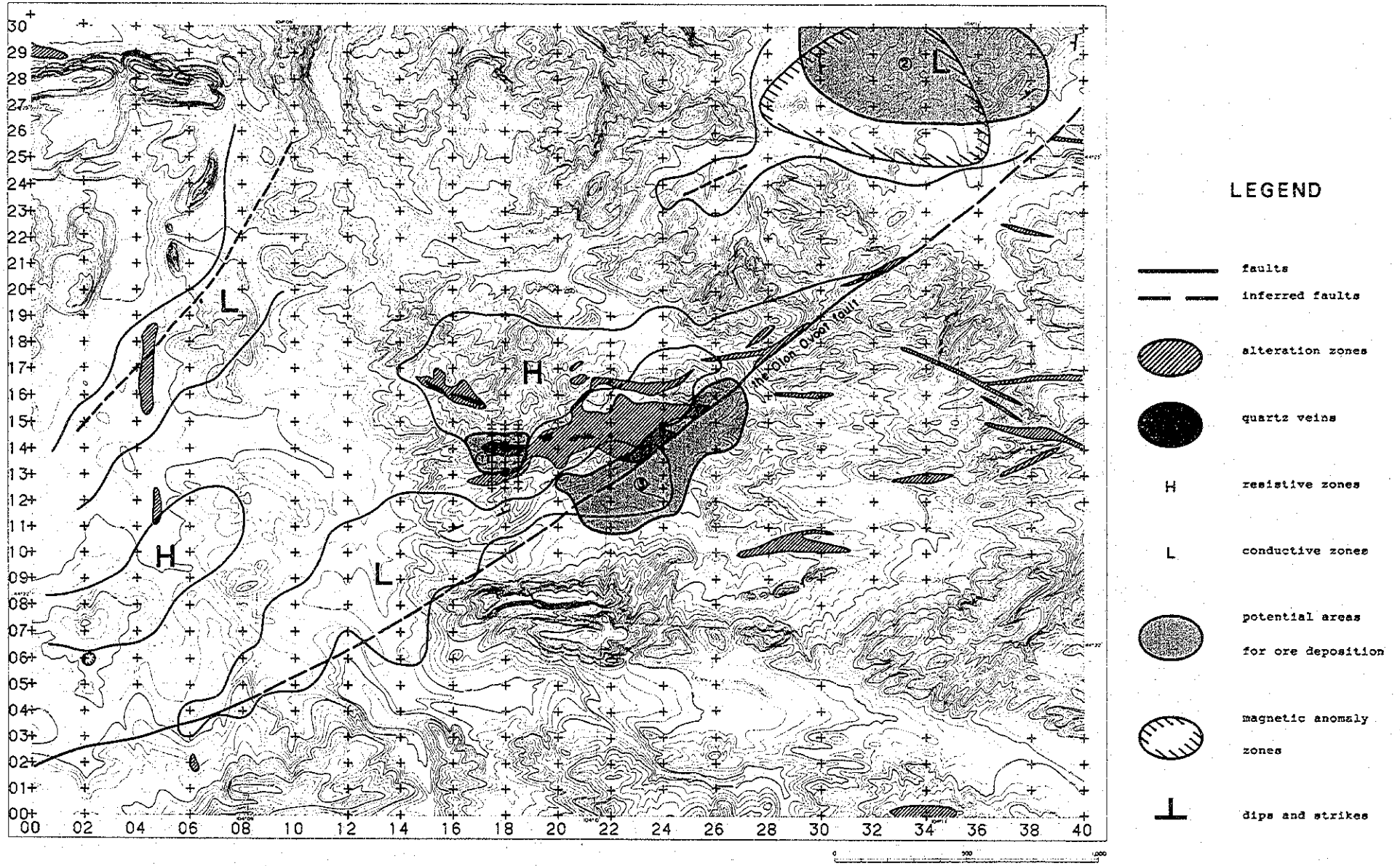

Fig. II-3-18 Map of geophysical interpretation

Chapter 4 Geochemical Survey

4-1 Purpose of the survey

The survey aims to clarify gold mineralization of the quartz veins of Olon Ovoot deposit and country rocks of quartz veins and to grasp extension, continuation and grade distribution of the mineral deposit.

4-2 Methods and contents of the survey

Geochemical survey was conducted covering an area of 1 km^2 of the Olon Ovoot deposit (Fig. II-4-1).

Base camp for the survey was located 5 km away from the deposit towards southeast direction. A survey team was organized by one Japanese geologist and one Mongolian geologist. Three survey teams were engaged in the work on survey lines. A total of 101 survey lines in the direction of magnetic N-S were set with a line interval of 10 m so as to crosscut the ore veins. Sample spacing on a survey line was, in principle, 2.5 m on quartz vein zone, 5 ~ 10 m on alteration zone and over 20 m on country rocks. Survey routes amount to 29.4 km including a base line survey and number of samples collected were 2,076. Field work was conducted making a route map with a scale of 1:1,000 using a pocket compass and measuring tape together with geochemical sampling.

Samples were selected to gather a fresh rock in situ and, in case of necessary, pitting was conducted. Trenching and drilling done by Mongolian before were also utilized for sampling localities.

Mineralized rocks and ore samples were provided for laboratory tests such as ore mineral analysis, microscopic observation of polished section, and measurement of homogenizing temperature of fluid inclusion Age determination adopting K-Ar method was conducted using muscovite in quartz vein and sericite from alteration zone adjacent to quartz vein.

Ore analysis was done for gold and silver with atomic absorption method. Detection limit for gold is 0.1 ppm and for silver 0.3 ppm.

Geochemical sample analysis was conducted for gold and silver using ICP method with detection limits of Au: 1 ppb and Ag: 0.2 ppm.

4-3 Survey results

4-3-1 Geology

Geology of the area is composed of Silurian and intrusive rocks (Fig. II-4-2).

Silurian is composed of crystalline schists of marine sedimentary origin and occupies majority of the area. The formation is composed of, in ascending order, siltstone, medium to fine-grained sandstone and greenschist which were intruded by medium to fine-grained diorite, medium to fine-grained granodiorite, basaltic andesite and trachyte. The formation changes its strike from NW-SE to NE-SW near the Olon Ovoot deposit and its eastern end is cut by the NE-SW running Olon Ovoot fault.

Diorite and granodiorite crop out in entire area as small intrusive bodies and basaltic andesite is found in the southwestern part of the area as a minor intrusive body.

The Olon Ovoot deposit is composed of quartz veins with in Silurian sedimentary rocks and assoirated intrusive rocks. Pyritized and silicified alteration oecurs in surrounding areas of quartz veins and along the fault zone.

Six zones of quartz veins, maximum width 20 m x extension 50 ~ 100 m, are distributed on the western side of the fault showing a chain of arcuate form. Total length of quartz veins

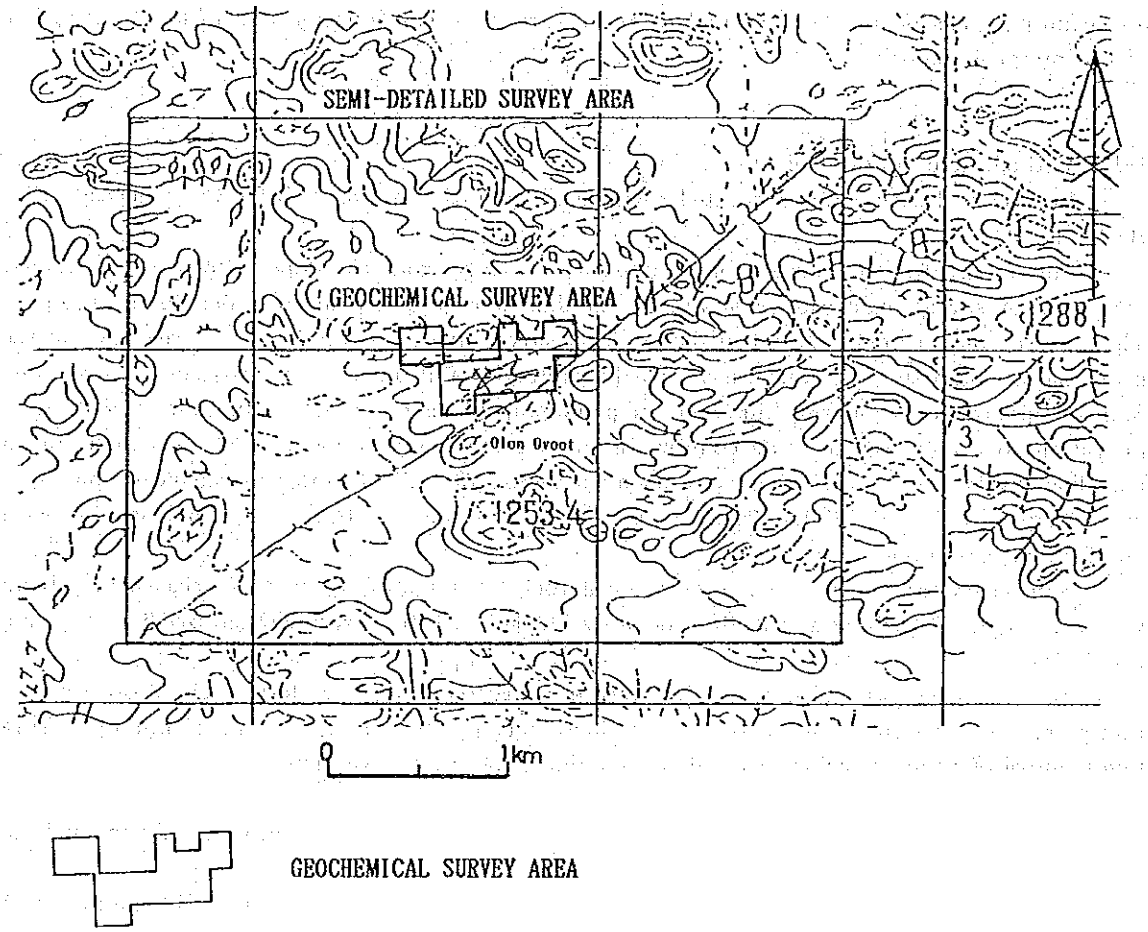

Fig. Ⅱ-4- 1 Location map of the geochemical survey area

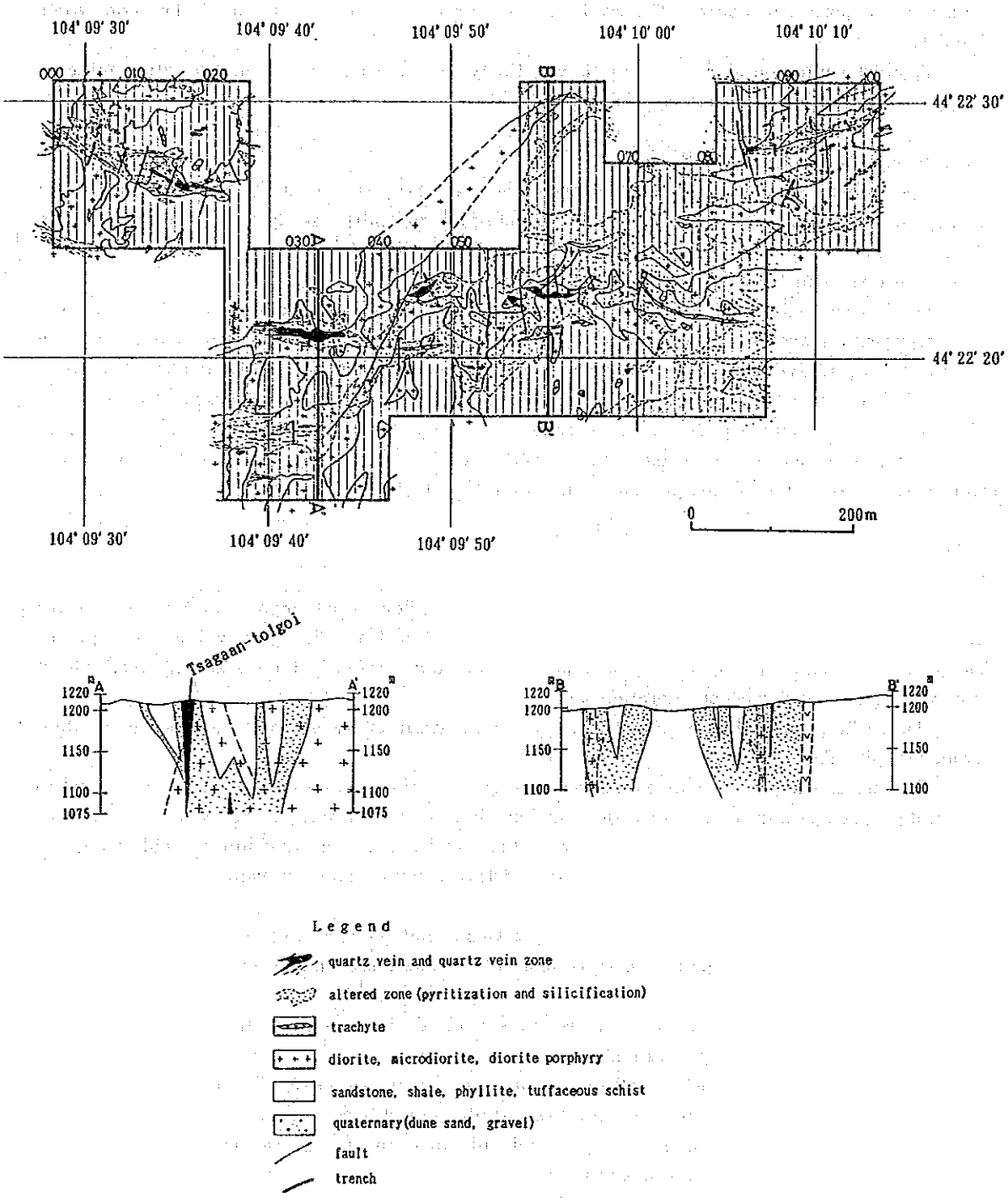

Fig. Ⅱ-4- 2 Geologic map of the geochemical survey area

reaches around 1,000 m at Olon Ovoot deposit. Aside from that near the deposit is developed a silicified-pyritized alteration zone with maximum width of 200 m.

Homogenization temperature of fluid inclusion is over 250°C at north and east of the Olon Ovoot deposit and below 250°C at Tsagaan Tolgoi where is the center of the Olon Ovoot deposit.

Age determination showes 283 ± 15 Ma, Early Permian age, from the alteration mineral along the quartz vein of Tsagaaan Tolgoi.

4-3-2 Results of Geochemical Survey

Geochemical anomaly maps of gold and silver were produced deciding threshold values with an aide of accumulated frequency distribution of gold and silver assay values (Fig. II-4-3 ~ II-4-5). Assay values were statistically analysed (Table II-4-1).

The results are summarized as follows:

Gold is concentrated in and near quartz veins and at Tsagaan Tolgoi highly concentrated gold occupies an area of 1,500 m^2 with 3.3 g/t of gold value. Other gold concentrations are encountered at quartz veins of both eastern and western extension and partly at alteration zone.

Silver is generally low grade and anomalous values were found at the central part of the Olon Ovoot deposit and nearby alteration zone.

Correlation between gold and silver is not admitted. No preferred concentration of gold and silver are observed in comparison with geologic units of the geologic map.

4-4 Consideration

The survey revealed that gold mineralization at Olon Ovoot deposit is concentrated to quartz veins and nearby parts confirming an area of 1,500 m^2 with gold value of 3.3 g/t at Tsagaan Tolgoi and other gold concentrated areas of quartz veins in both east and west side of surveying area and a part of alteration zone.

As a whole, a total area of 2,500 m^2 with gold grade of 3.2 g/t will be expected at Olon Ovoot deposit (Table II-4-2).

Spacing of sampling points in crosscutting quartz vein is more than 2.5 m apart. Due to this wider spacing, narrower quartz veins at both east and west side of the Olon Ovoot deposit were not able to demarcate mineralized areas. Judging from the fact that higher gold values are sporadically admitted in these zones, a further detailed survey may warrant an increase of ore blocks.

Grain size of gold is fairly coarse at Olon Ovoot and, in rare occasion, even country rock near quartz vein produces gold. These facts might suggest secondary enrichment occurred in this area.

As to gold mineralization in the country rock, it is necessary to pay attention with relationship to silicified-pyritized alteration.

Scarcity of silver in the Olon Ovoot deposit is an essential character of the mineralization, since the deposit contains few sulfide minerals.

Taking these findings in mind, it is advisable to conduct exploration of the Olon Ovoot deposit for lateral and vertical continuation.

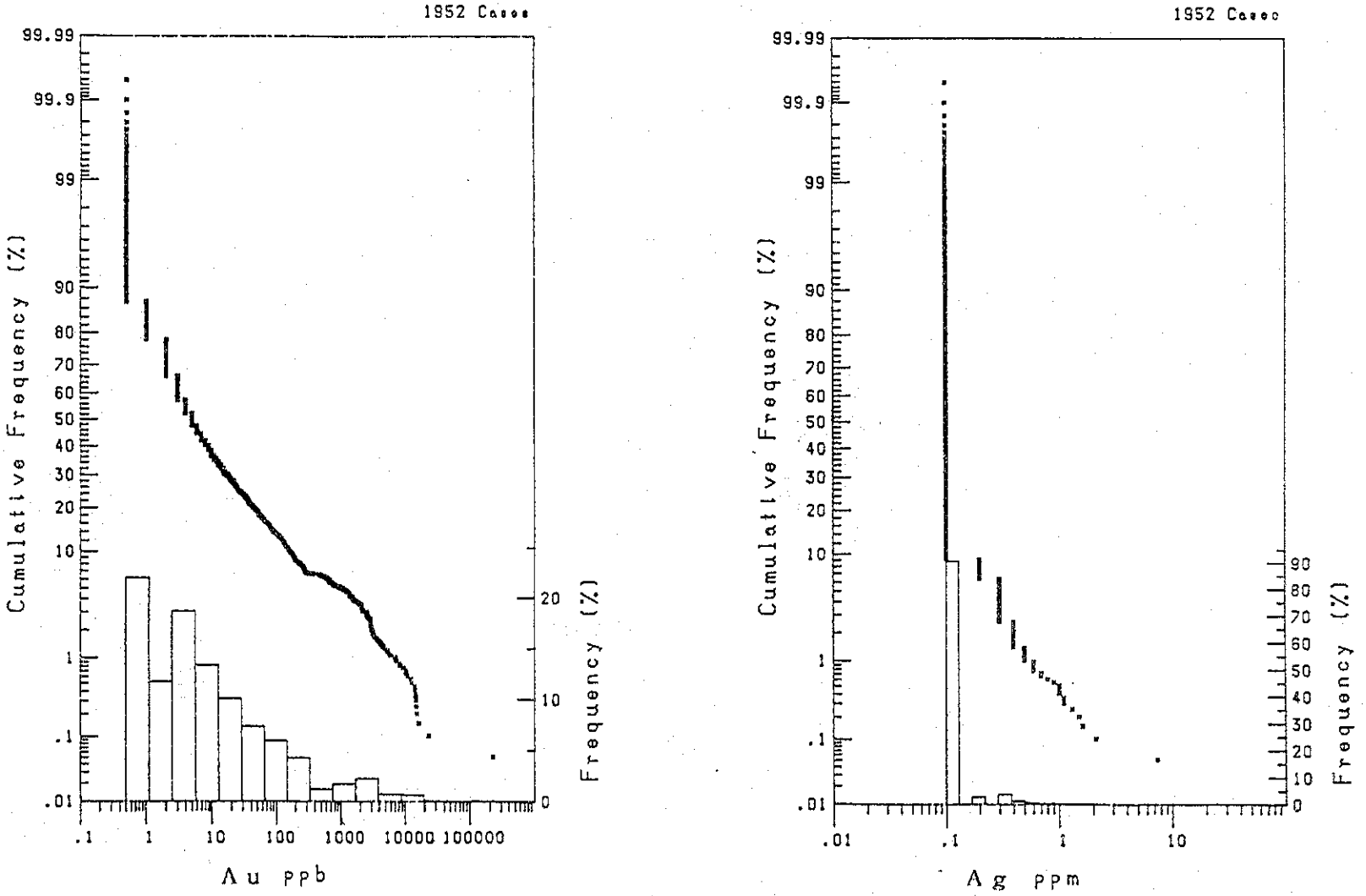

Fig. Ⅱ-4- 3 Cumlative frequency curves of assay results in geochemical survey area(Au, Ag)

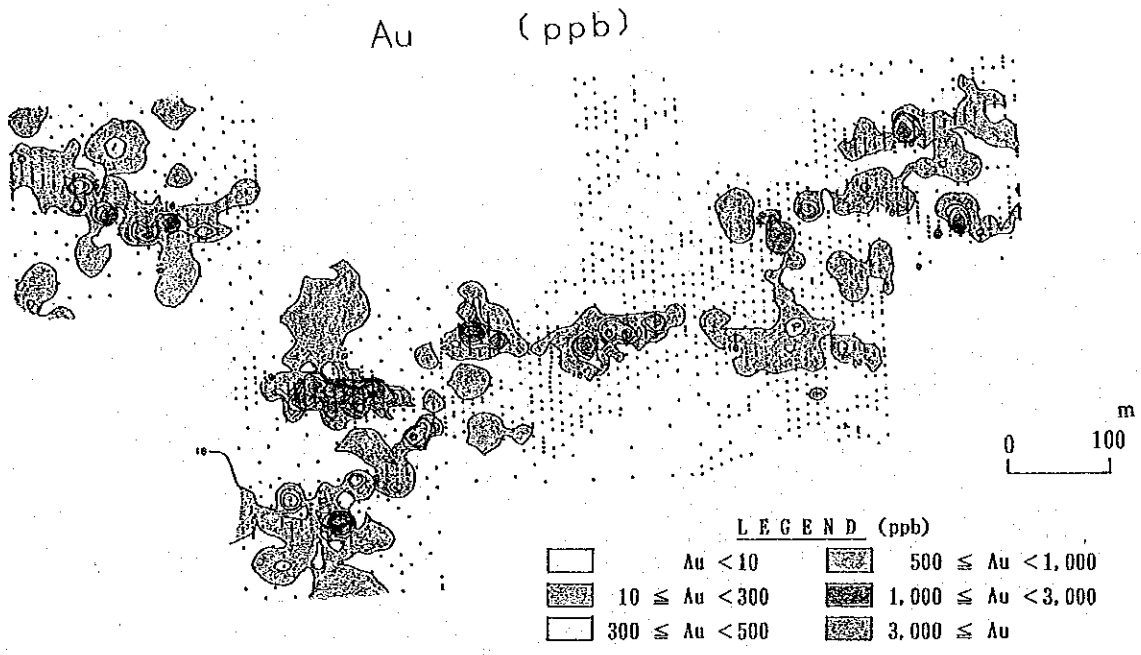

Fig. Ⅱ-4- 4 Distribution of gold in the geochemical survey area

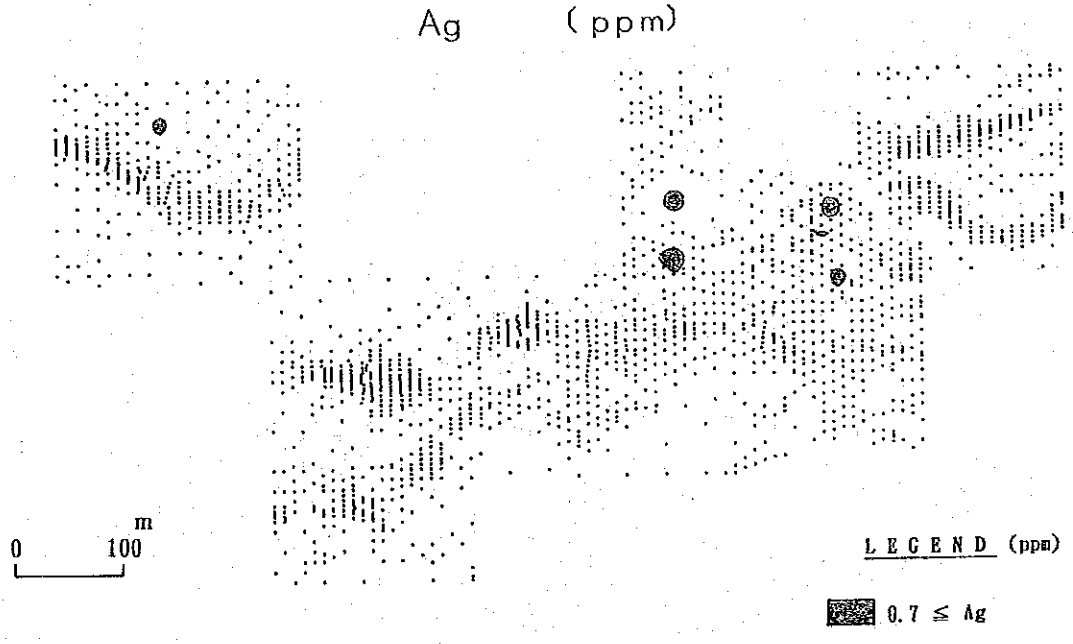

Fig. Ⅱ-4- 5 Distribution of silver in the geochemical survey area

Table Ⅱ-4- 1 Statistical numbers on gold and silver in the geochemical survey

	Au	Ag
試料数	1952	1952
最大値	223000	7.3
最小値	0	0.1
平均	365.13	0.13
Auとの相関係数	1	0.1658**

**: 有意(有意水準=0.001)

Table Ⅱ-4- 2 Ore-blocks and ore-grade of the Olon Ovoot deposit

Block No.	Size (㎡)	Average grade (Au g/t)	Numbers of samples(pcs)	N o t e
1	1,500	3.3	60	Tsagaan Tolgoi(massive quartz ～quartz vein)
2	500	2.3	15	150 m west from Tsagaan Tolgoi(wide quartz vein)
3	140	7.3	5	130 m south from Tsagaan Tolgoi(qz v and host rock)
4	90	1.9	4	630 m northeast from Tsagaan Tolgoi (qz v)
5	250	2.0	3	280 m east from Tsagaan Tolgoi (wide qz v)
6	50	2.7	5	250 m～330 m northwest from Tsagaan Tolgoi (qz v)
Total	2,530	3.2	92	

Note: Numbers in this table should be taken for "Potential" because of the number of the analysed samples are too few to evaluate gold deposit. Closer sampling is required to consolidate the workable area and the ore grade.

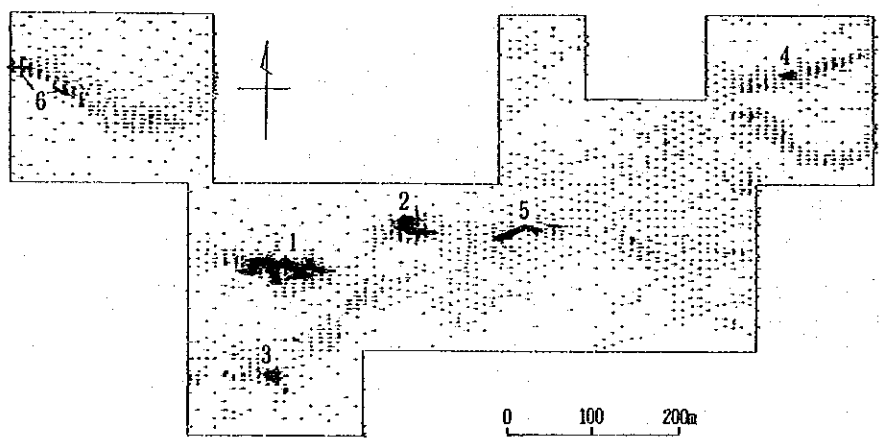

Chapter 5 Consolidated discussions on the survey results

5-1 Mineralization model of the Ulziit District

The survey results revealed that there are several epochs of gold mineralization in the Ulziit District: Early Permian as the case of Olon Ovoot, Onh and North Harmagtai, Cretaceous at Sologoi and possibly late Carboniferous at Olon Ovoot. Paying attention to the above-mentioned phenomena, a model on gold mineralization in the area was drawn taking consideration of geological setting, homogenization temperature of fluid inclusion and alteration mineral facies (Fig. II-5-1).

Locations of each mineral indication represent degree of erosion up to present time.

Geological and ore depositional characters of each mineral indication will be explained by this model without much inconsistency and the following mineral indications will be further exploration targets to verify existence of blind gold mineralization: Soirig, Sologoi, North Harmagtai, western part of Tsagaan Uula, West of Onh and North Olon Ovoot.

Homogenization temperature of fluid inclusion study revealed that the temperature distribution pattern shows a typical normal distribution from the samples of Soirig and North Harmagtai which means mineralization occurred only once, on the contrary several modal distribution patterns are observed at Olon Ovoot, Dugshih and Sologoi which means repeated mineralization might ocuur in those areas. Hydrofracturing texture is often observed in the quartz veins and silicified rocks of the Ulziit District. The texture suggests that a boiling of ore-forming fluid occurred.

Gold mineralization model should explain the above-mentioned phenomena and in order to specify the loci of mineral concentration within ore bodies, further detailed survey is necessary and this leads to produce more precise model of mineralization.

Integrated and consolidated appraisal were given to the main mineralization in the Ulziit District. As the result, many hopefull ore-indications were extracted in Soirig, Sologoi and North Harmagtai areas aside from Olon Ovoot deposit (Table II-5-1).

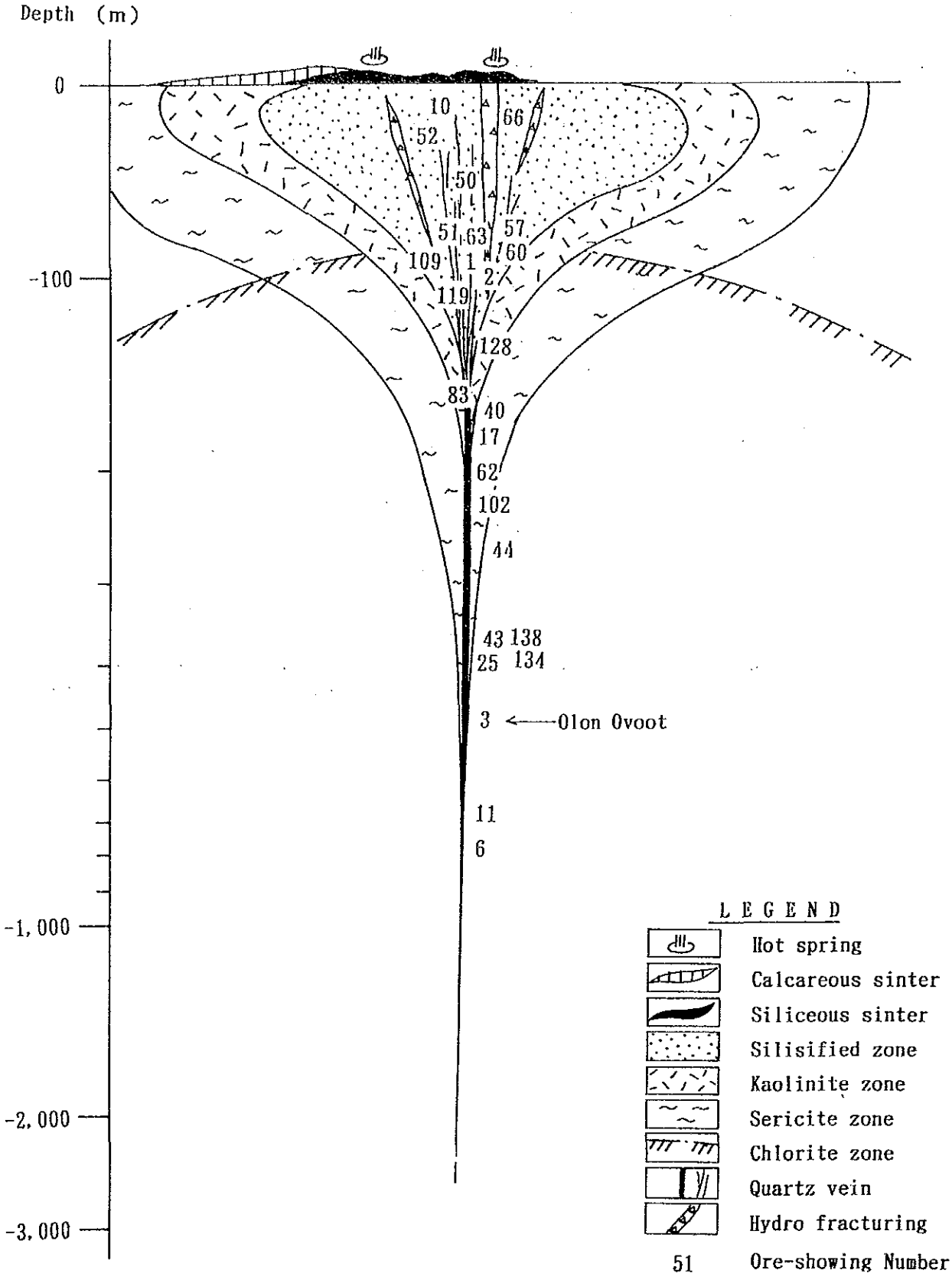

Fig. Ⅱ-5-1 Erosion levels of the ore-showings in the Ulziit area

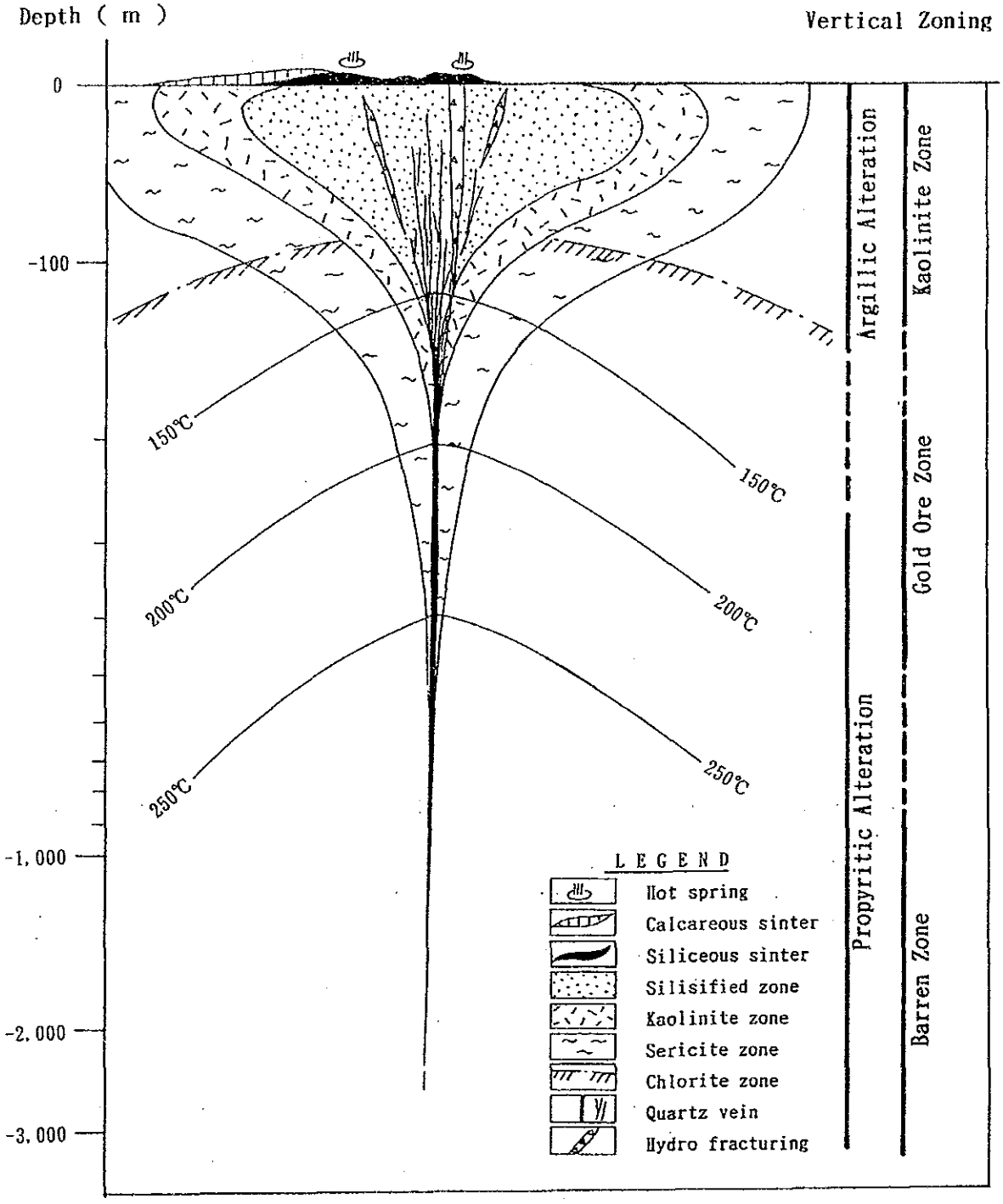

Fig. II-5-2 Schematic geochemical profile of the gold ore-showings in the Ulziit area

Chapter 6 Previous data analysis survey

6-1 Purpose of the survey

The survey is aimed to grasp regional geology of the area and to clarify relation between geology and mineralization for picking up potential areas of further exploration by means of collecting, reading and analysing all the available data on the exploration of the Dornod District.

6-2 Method and contents of the survey

The survey was conducted by three Japanese geologists and the Mongolian counterparts at Ulaan Baatar in a week during Nadam festival. Study was focussed on the eight geophysical prospection reports of the area provided by Mongolian counterpart, followings are the contents of the survey:

a. Period when the survey was conducted, implementing agency, purpose of the survey and target area.
b. Survey method applied
c. Results of the survey
d. Follow-up survey if any and the survey results
e. Extracting promising areas

6-3 Survey results

Previous survey reports conducted from 1952 to 1990 were provided and a list of the reports is shown in Table II-6-1. Results are as followings.

6-3-1 Geology and geologic structure of the Dornod District

1. Geology

Geology of the District is composed of Upper Proterozoic, Paleozoic, Mesozoic and Cenozoic age.

Upper Proterozoic-Lower Paleozoic formations are composed of various metamorphic rocks derived from green to black shale of marine origin and crop out in the northern part of the area extending NE direction.

Paleozoic formations are composed of Devonian greywacke and acidic volcanics of Permian-Triassic age. The former crops out surrounding Upper Proterozoic in the northern part of the District and the latter crops out covering whole of the central part of the District.

Mesozoic formation occupies a wide area of the central part of the District and is composed of Triassic sedimentary rocks and basalt, andesite, trachyandesite and trachyte of Late Jurassic to Early Cretaceous terrestrial products.

Cenozoic formations are Paleogene-Neogene occupying the central valley of the District and Quartenary developed at the northernmost part of the District.

2. Geologic structure

The Dornod District is located in the Central Mongolian fold belt. The structure of the District is characterized by NE-SW stretching Paleozoic formations and Mesozoic Choibalsan sedimentary basin which was formed in the central part of the District.

Choibalsan sedimentary basin shows an ellipsoid, diameter of E-W 180 km and N-S 150 km, with its center around 50 km northwest of Choibalsan city. The basin is covered with thick terrestrial formations with intercalation of coal seams and is surrounded by basic

Table II-6-1 List of previous survey works in the Dornod Area

No.	Reg. No.	Survey Method	Performance	Age	Purpose	Conductor	Results
1	1264	Gravity Survey line span 3 ~4 km point distance 1km gravimetorГКА No. 27 accuracy 0.5mgal	9,800 km² (whole Choibalsan basin)	1952	Oil	Ministry of Petroreum Industry, USSR ИВАНОВА	①Gravvity map(1:100,000 2mgal intvl ②discovery of Sumin-nuur basin ③no density data
2	1762	Aero-magnetic Surv. line span 1.8 km flight alt 200±20m magnetmeter AMM-13 navigation topo map	205,000 km² E area 156,000km² W area 49,000km²	1966 ~ 1967	general prospective	Ministry of Mining, MPR. В.И.Вдовенкин А.И.Попов	①Magnetic anomaly map 1: 200,000 1:1,000,000
3	2060	Gravity Survey line span 3 ~4 km presumed D. 2.67 gravimetor ГКА-7Т	5,700 km² measuring 738 pts Ulz R. to Imalkin R.	1972 ~ 1973	Sn, W granite pluton-greisen	MPR-USSR JV	A blind pluton was predicted near by Chuluun Haraat. no density data
4	2447	Aero γ-ray1: 25,000 Auto γ-ray1: 10,000 〃 1: 25,000 〃 1:200,000 Man γ-ray Radio Act.1: 10,000 Trench	32,600 km² 647 km² 2,392 km² 1,062 km² 5,291 pts 71 km² 168,800 m³	1972 ~ 1974	U	Ministry of Geology, USSR / MPR JV	Aero- γ-ray map 1: 25,000 Aero-magnetic map 1: 50,000 1:200,000 83 anomalies were extracted.
5	2416	Gravity Survey Car borne Man borne	600 km² 487 km² 113 km²	1976 ~ 1977	U	Ministry of Geology, USSR / MPR JV	Many Uranium ore-showings were discovered.
6	2459	Root Geol. Surv. Geochemical Surv. Trenci Boring γ-logging Radio Activation M. Erectric(I.P., S.P.) Car-Magne(1/10,000, 1/25,000)	2,912 km 26,734 pcs 287,904 m³ 113,929 m 112,929 m 106,890.5 m 402.6 km 563 km²	1986 ~ 1989	Poly-metal	Ministry of Geology, USSR / MPR JV	Ore-reserve of Ulaan and Muhar was increased. Avtartolgoi ore deposit was discovered.
7	4441	Geol Surv. 1:50,000 〃 (Root) Geochemical Survey Panning Trench Pit Boring Magnetic Survey	1,250 km² 17,115 km 42,292 pcs 3,708 pcs 456,474 m³ 277.5 m 2,226.1 m 644 km	1986 ~ 1990	Poly-metal	Mongolia O. Gombobaatar B. Tsogtsaihan	Geologic map (1: 50,000) Many polymetallic ore deposit such as Altan Tolgoit, Salhiit, Umnug were discovered.
8	4555	Geol.Surv. 1:200,000 〃 1: 50,000 Geophys-Geochm cplx	40,000 km²	1989 ~ 1990	Poly-metal, Ag, Sb, F	Minstry of geo-	discovery of Baits (poly metal) and Huhur(Cu-Au, Cu-Sn)

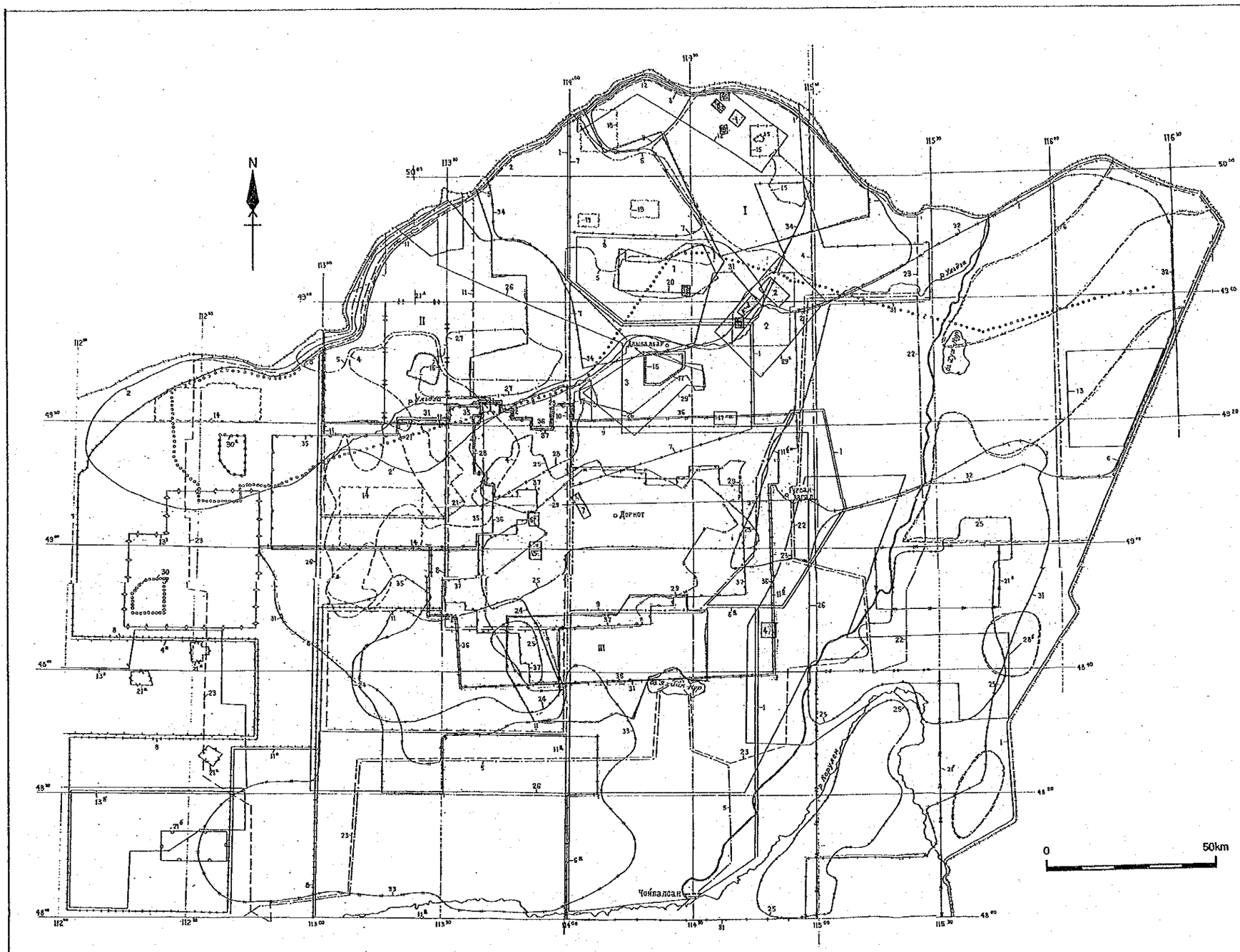

No.	Contor	Author	Year	Scale
1		Murinov, N.A. et al.	1943	1:1,000,000
2		Jelubonokii, U.O.	1943	1:1,000,000
3		Kalenos, A.D. et al.	1944	1:200,000
4		Ivanov, A.H., Anpilov, M.A	1945	1:200,000
4 a		Ponsanov, N.D.	1945	1:200,000
5		Lâenko, S.T. et al.	1952	1:200,000
6		Darilov, B.L	1953	1:200,000
6 a		Kirekhev, V.D.	1953	1:200,000
7		Byzunov, U.S., Alekseev, T.A.	1958	1:200,000
8		Bleguvserov, V.A. et al.	1968	1:200,000
9		Angas, J. et al.	1972	1:200,000
10		Togoh, D. et al.	1973	1:200,000
11		Togoh, D. et al.	1974	1:200,000
11 a		Maslennikov, H.A. et al.	1954	1:200,000
11 б		Maslennikov, H.A. et al.	1953	1:50,000;1:100,000
12		Borkov, F.Ts. et al.	1959	1:50,000
13		Lavitov, V.I.	1953	1:50,000
13 a		Norovsambuu, Ts. et al.	1981-84	1:50,000
13 б		Norovsambuu, Ts. et al.	1984-86	1:50,000
13 в		Chuluunsuh	1984-87	1:50,000
14		Varlamov, V.A., Gorobov, V.A.	1961	
15		Vanzegch, J., Baheb	1968-69	
16		Anufiev, I.F., Sokolov, K.M., Nyam, B.	1969	reconnaissance survey
17		Subbastar, H., Altangeroks, Nyaru, B.	1970	and evaluation
18		Zahal, T., Lavirenko, L.	1970	
19		Kuznetsov, V.A., Obolenskii, A.A.	1977	
20		Temursuh, Z., Sumiyana, D., Udina, A.	1980	ditto
21		Dolgor, Ya. et al.	1983	ditto
21 a		Norovsambuu, Ts.	1981-82	1:10,000
21 б		Avid, N.	1980-81	1:25,000
21 в		Gombobastar, Sanjsugar, Terebilo	1986	1:50,000
21 г		Gerbastar, Arslin, Snetkov, M.V.	1988	1:50,000
21 д		Anbbayar et al.	1986	1:50,000
		Airborne Geophysical Map		
22		Markov, A.I., Chistsov, L.D.	1981	1:200,000
23		Markov, A.I., Chistsov, L.D.	1970-80	1:25,000
		γ -ray Spectrometry Survey		
24		Samovich, D.A., Chirtsov, L.D.	1970-74	1:200,000
25		Chirtsov, L.D., Malavich, D.Z.	1971-75	1:10,000-1:25,000
		Geological Map		
26		Vladimirskii, G.M. et al.	1976-79	1:200,000
27		Lecherkin, U.N. et al.	1975-76	1:50,000
28		Gusev, A.I., Roguzenok, R.K. et al.	1976-77	1:50,000
29		Pecherkin, U.N. et al.	1972-80	1:50,000
29 a		Mironov, U.B. et al.	1978-88	1:50,000
29 б		Soloviev, N.S. et al.	1987-89	1:200,000
		Revised Survey Work		
30		Tsekin, V.V., Tsekina, A.I.	1974-85	1:100,000
30 a		Margui, A. et al.	1971-76	1:25,000
		Gravimetric Map		
31		Glyanko, N.K., Kozmetsov, A.G., Levitskaya, A.I.	1982-85	1:500,000;1:200,000
32		Ivanova, B.A. et al.	1952	1:200,000
33		Gerrublat, T.M. et al.	1954	1:200,000
34		Zorin, U.A., Tumurov, E.H.	1973	1:200,000
35		Tudev, Lurevdorj, Dagvadorj et al.	1981-83	1:100,000
36		Zlobin, V.P., Semenov, G.G., Ivannikov, V.N. et al.	1974-83	1:200,000;1:50,000

1 — Geologic mapping scale 1:50,000
geochemical sampling, trench and drilling
1 - Arshanskaya, 2 - Uldeinskaya (gravity survey, drilling),
3 - Dashibalbarskaya (short drilling)

I — Geologic mapping scale 1:200,000
I - Yujno Aginskaya, II - Turganskaya,
III - Yablin Nurskaya

Reconnaissance survey
scale 1:500,000 - 1:1,000,000

After Ministry of Geology, USSR (1990)
"- North Choibalsan Area -
Location Map of Geological and Geophysical Study Area"

Fig. Ⅱ-6- 1 Distribution map of the previous survey works in the Dornod area

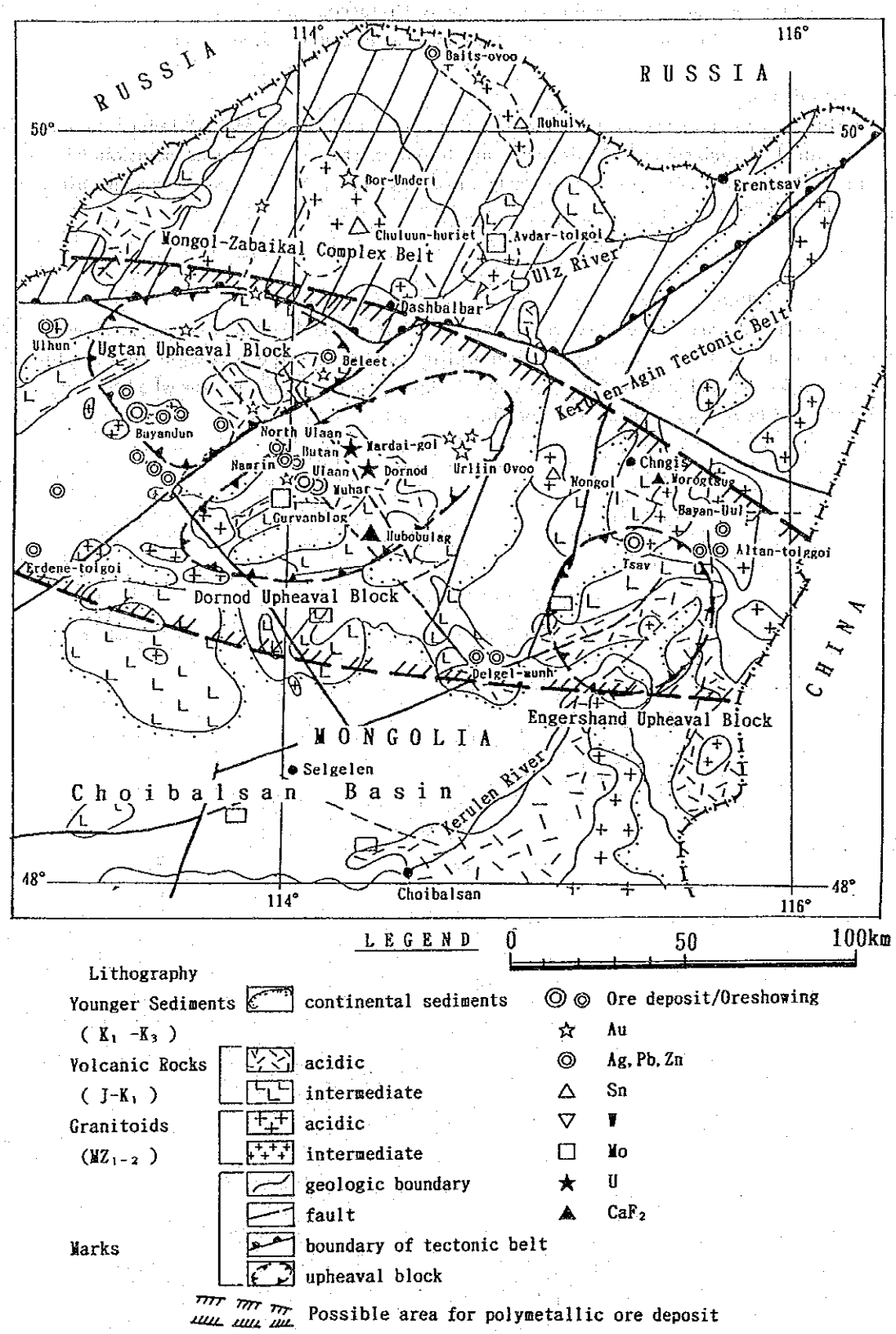

Fig. Ⅱ-6-2 Interpreted map of the existing data

to acidic volcanics of Late Jurassic to Early Cretaceous age.

The structure is clearly represented by a gravimetric survey result.

6-3-2 Ore deposit

Mineral deposits such as polymetallic deposits of Tsav, Ulaan, Muhar, Delger-Munh, Salhiit and Bayan-Uul and some gold deposits are found in the District in association with severe volcanic activities of Late Jurassic to Early Cretaceous age. Main mineral deposits are marked on the Fig. II-6-2.

6-4 Consideration

The central part of the District is covered widely with Mesozoic volcanic products. There is a high potentiality of existing polymetallic and gold mineralization in volcanic field between Bayandun and Bayan-Uul, especially in high gravity anomaly zone which is located at a periphery of Choybalsan sedimentary basin.

Part III CONCLUSION AND RECOMMENDATION

Chapter 1 Conclusion

1-1 The Ulziit District

The followings are conclusions of the survey in the Ulziit District.

1-1-1 Olon Ovoot deposit

1. The Olon Ovoot deposit is composed of six quartz vein zones, with a maximum width of 20 m x extension of 50 ~ 150 m, and a total length of quartz vein zones reaches 1,000 m.

2. The deposit contains minable grade of gold.

3. Gold mineralization is found mainly in quartz veins and a part of alteration zone.

4. An area of 1,500 m^2 with 3.3 g/t of gold is demarcated on the surface.

5. Minable grade of gold are sporadically found in quartz veins with vein width of less than 2.5 m and by adding a further detailed survey to those parts will increase area of minable ore.

6. Geophysical survey revealed that the Olon Ovoot deposit might continue downward a few hundred meters with a steep dip of 80° as a high resistivity zone.
   A great amount of ore reserve is expected the depth of the Deposit.

7. Quartz vein can be picked up promptly and clearly as a high resistivity zone by adopting TEM with proper spacing of measurement to the size of a target.

8. Geological and mineralogical characters of gold concentration is as follows:
   ① Absolute age of mineralization is 283 ± 14 Ma for muscovite in quartz vein and 301 ± 15 Ma for clay mineral from a boundary of quartz vein.
   ② Homogenization temperature of fluid inclusion ranges from 170°C to 250°C at part of gold concentration,
   ③ Alteration facies of the gold mineralized quartz vein is sericite-chlorite or chlorite. Minor amount of kaolinite occures near around.
   ④ No clear correlation is found between gold and other assay elements.

1-1-2 Reconnaissance survey

1. A lot of big quartz veins and silicified rocks were found in Soirig, Sologoi and North Harmagtai area.

2. Above-mentioned mineral indications are low grade on the surface but the following findings will warrant further exploration to verify blind gold mineralization of the areas.
   ① Age of mineralization is 286 ± 15 Ma for clay mineral of quartz vein boundary at Sologoi and 274 ± 14 Ma for clay mineral.
   ② Quartz veins are mostly composed of milky white quartz and most of the homogenization temperatures of the fluid inclusions are below 220°C.
   ③ Total accumulated volume of hydrothermal quartz of the Ulziit District is as big as over five hundred million tons.

Table Ⅱ-1-1 Feasibility evaluation of major ore showings in Ulziit Area

Area	No.	Description					Evaluation						Note
		PVSi x 10^3 t	POG g/t	D_{250} m	Form M/V	Dv Tm^3 km^2	PVSi	POG	D_{250}	Form	Dv	TOTAL SCORE	
Olon Ovoot	1	180	3	300	V	150	2	2	2	1	2	16	Horimt Hudag
	2	200	3	300	V	160	2	2	2	1	2	16	N. Olon Ovoot
	3	3,670	3	-50	M/V	3,000	3	2	5	2	3	180	Olon Ovoot
	6	1,102	3	-310	V	600	2	2	0	1	2	0	Unegt Uul
Tahilga Uula	—	—	—	—	—	—	—	—	—	—	—	—	—
Tsagaan Uula	10	1,290	3	400	V	700	3	2	1	1	2	12	Z. Hailhan U.
	11	6,610	3	400	M/V	1,000	3	2	1	2	3	36	
Dugshih	17	470	3	230	V	1,910	2	2	3	1	3	36	
	25	150	3	10	V	600	2	2	5	1	2	80	
	40	165	3	230	V	1,100	2	2	3	1	3	36	
	41	440	3	*	V	3,000	2	2	*	1	3	≦ 12	
Onh	43	730	3	50	V	400	2	2	5	1	2	40	Onh
	44	14,700	3	190	V	3,400	4	2	4	1	3	96	N. Onh
Soirig	50	1,100	3	350	V	6,000	3	2	2	3	3	108	N. Munh Ts. T
	51	70,800	3	350	V	44,500	4	2	2	3	4	192	Munh Ts. T.
	52	9,200	5	380	M/V	3,600	3	3	2	2	3	108	Zalaa Uul
Sologoi	57	49,000	5	350	M/V	1,100	4	3	2	2	3	144	Dersen Us H.
	60	30,600	5	350	M/V	890	4	3	2	2	2	96	Morit
	62	29,400	3	210	M/V	860	4	2	3	1	2	48	Futur Us
	63	27,500	3	350	V	3,200	4	2	2	2	3	96	Ulziit Ovoo
	64	19,800	3	*	M/V	8,500	4	2	*	3	3	≦ 72	Sologoi B.
	66	107,000	3	430	M	10,100	5	2	1	3	4	120	H. Ts. T.
	68	29,400	3	*	M	10,900	4	2	*	3	4	≦ 96	
	69	6,100	3	*	M	5,000	3	2	*	3	3	≦ 54	
	70	18,300	3	*	M	10,000	4	2	*	3	4	≦ 96	
	73	13,700	3	*	M	35,000	4	2	*	3	4	≦ 96	
Undur Uda	—	—	—	—	—	—	—	—	—	—	—	—	
North Harmag-tai	83	1,470	3	260	V	660	3	2	3	1	3	54	
	84	6,120	3	*	M	10,000	3	2	*	3	4	≦192	
	102	2,700	3	190	M/V	44,000	3	2	4	2	4	192	
	109	4,200	3	310	V	1,750	3	2	2	1	3	36	
	119	2,400	3	300	V	2,500	3	2	2	1	3	36	
	128	3,300	3	290	V	4,800	3	2	3	1	3	54	
	134	4,700	3	0	M	5,600	3	2	5	3	3	270	
	138	14,700	3	80	M	10,400	4	2	5	3	4	480	
	141	6,120	3	*	M	1,670	3	2	*	3	3	≦ 54	

PVSi: Potential Volume of Silica (in thousand tons)
POG: Potential Ore Grade (g/t)
D_{250} : Depth of the 250℃ line of homogenization temperature of the fluid inclusions from the ground surface (m)
Form: Massive (M: Width≧ 5 m) or Vein (V: Width ≦5 m)
Dv: Density of veins (in thousand m^3 / km^2)
*: No data
—: Nothing worthy of evaluation

Total score = PVSi×POG ×D_{250} ×Form×Dv

Score allocation of the factors

Score	PVSi t	POG g/t	D_{250} m	Form M/V	Dv m^3 / km^2
5	$10^6 \leq n$	30≦ n	0≦ D <100		$10^5 \leq$ Dv
4	$10^5 \leq n < 10^6$	10≦ n <30	100≦ D <200		$10^4 \leq$ Dv <10^5
3	$10^4 \leq n < 10^5$	5≦ n <10	200≦ D <300	H	$10^3 \leq$ Dv <10^4
2	$10^3 \leq n < 10^4$	3≦ n <5	300≦ D <400	M/V	$10^2 \leq$ Dv <10^3
1	$10^2 \leq n < 10^3$	1≦ n <3	400≦ D <500	V	$10^1 \leq$ Dv <10^2
0	$n < 10^2$	n <1	500≦ D <-200		Dv <10^1

④ Wall rock alteration is represented by sericite or chlorite–sericite facies.
⑤ Massive silicified bodies are considered to have been formed near the surface.
⑥ Siliceous and calcareous sinters formed on the surface are partly observed.
⑦ Higher the homogenization temperature (220°C), the greater the gold value at Morit mineral indication in the Sologoi area.
⑧ Hydrofracturing texture which is admitted as a favorable condition for gold concentration is widely seen.
⑨ Fluid inclusion study revealed that boiling of ore–forming fluid occurred in the areas.

3. There are possible blind gold mineralizations at Onh and Tsagaan Uula areas.

4. Mineral indications found in Tahilga Uula, Dugshih and Undur Uda are too small and scarce to be an exploration target.

5. Unexplored large scale mineralization is expected in the Ulziit District.

1-1-3 Remarks

Geophysical prospection revealed that a low resistivity zone exists at 2 km northeast of the Olon Ovoot deposit. The anomalous zone might suggest a presence of magnetite and/or pyrrhotite–bearing skarn type deposit or sedimentary massive sulfide deposit, judging from the following facts:

1. Presence of Devonian limestone.

2. Presence of small intrusives of diorite and granodiorite.

3. Location on the fault which is accompanied by hydrothermal activity.

4. Presence of skarn ore with green copper minerals in limestone near the anomaly.

5. Location in pelitic crystalline schist overlying greenschist. (possibility of strata–bound massive sulfide deposit)

6. The area is accompanied with a strong magnetic zone to affect the reading of survey instruments.

The anomaly takes a size of E–W 600 km × N–S 600 m below the surface of 50 ~ 100 m and extends toward NE to the outside of surveying area.

1-2 Dornod District

1. Area from Bayandun to Ulaan, Deler–Munh, Tsav and Bayan Uul form the most important polymetallic deposit belt in the Dornod District. Mineralization occurred together with igneous activity of Late Jurassic to Early Cretaceous age.

2. Adjacent to the south of the above–mentioned belt lies Choibalsan sedimentary basin buried with various igneous rocks of Late Jurassic to Early Cretaceous age.

3. Choibalsan sedimentary basin especially between Bayandun and Bayan Uul might hide polymetallic ore deposit.

4. Cretaceous formation with intercalation of coal seams is low in solidification, therefore, there exist a density difference between Cretaceous formation and underlying Jurassic to Cretaceous igneous rocks.

5. High gravity anomaly found at the northern part of Choibalsan sedimentary basin might show blind polymetallic mineralization.

6. Above-mentioned area was covered with Russian gravity Survey during 1974 to 1983 and gravity maps on a scale of 1:50,000 and 1:200,000 were compiled but no report on the gravity survey was handed over to Mongolian authority.

Chapter 2 Recommendation

2-1 Ulziit District

2-2-1 Olon Ovoot deposit

The following survey is advisable to secure ore reserves in the deposit.

1. Drilling to confirm a deep extension of the deposit which is proposed by geophysical survey.

2. Further detailed vein survey to the both sides of the deposit.

3. Geophysical survey to confirm lateral extension of the quartz veins.

4. Detailed vein survey in the northwestern part of the area.

2-1-2 Reconnaissance Survey

1. Regional mineral indication survey covering wide area from Ulziit District to Tsagaan Svraga.

2. Appraisal survey for mineral indications encountered at Soirig, Sologoi and Harmagtai North with geological, vein-character, analysis of ore, homogenization temperature measurement, alteration and age determination survey.

2-1-3 Remarks

As to geophysical anomaly found at 2 km northeast of the Olon Ovoot deposit, the following additional geophysical survey is recommended:

1. TEM-method to grasp a lateral extension of the zone of low resistivity.

2. Magnetic survey to verify an extension of high magnetic anomaly.

2-2 Dornod District

Blind deposit of polymetallic type are expected in the Dornod District and gravity survey is most suitable method at the beginning of exploration to this type of deposit. It is therefore the most advisable to obtain previous survey data and report done by Russian survey team, and to make through study of them for planning further step of survey to this District.

BIBLIOGRAPHY

I PUBLISHED LITERATURE

Academy of Research and Science MPR, Bureau of National Geodesy MPR et al. (1990) : Basic Atlas of the Mongolian People's Republic. Ulaan Baatar-Moskva (in Mongolian).

Academy of Science MPR (1990) : Information Mongolia. James C.V. Ed., Pergamon Press, London, 505p. (in English).

Metal Mining Agency of Japan (1991) : Geology and ore deposits in Mongolian People's Republic. Mineral Resources Information Center (in Japanese).

Ministry of Geology USSR, Scientific Technological Laboratory on Geology of Foreign Countries and Ministry of Geology and Mining MPR (1977) : Geology of Mongolian People's Republic, vol. 3, Usefull Minerals., N. A. Marinov,, R. A. Hasin, Ts. Hurts Ed., 'Nedra', Moskva, 703p. (in Russian).

Parker, H. and Gealy, W. K. (1985) : Plate tectonic evolution of the Western Pacific-Indian Ocean region. Energy, vol. 10, p. 249-261 (in English).

Taira, A. and Tashiro, M. (1987) : Late Paleozoic and Mesozoic accretion tectonics in Japan and Eastern Asia. Taira A. and Miyashiro M. Eds. Historical biogeography and plate tectonic evolution of Japan and Eastern Asia. Terra Scientific Publishing Co., Ltd., Tokyo, p. 1-43 (in English).

Miyashiro, A. (1979) : An Outline of the tectonics of Asian continent. Miyashiro A. Ed. Iwanami Kooza Earth Science 16, Iwanami-shoten, p. 237-261 (in Japanese).

II UNPUBLISHED LITERATURE

A. DORNOD district

1. No. 1264 Ivanova, E. A. (1953): Report on the result of the gravimetric survey at the Dornod aimag, Mongolian People's Republic in 1952. Geophysical Expedition of the Ministry of Oil Industry of USSR, Moscow, 58p. (in Russian).

2. No. 1762 Blyumentsvaig, V. I., Popov A. I. (1966-1967): Report on aeromagnetic survey on the territory of Mongolian People's Republic in accordance with the contract No. 1495. Ministry of Geology, Mongolian People's Republic, 270p. (in Russian).

3. No. 2060 Zolin, U. A., Turutanov, E. H., Novoselova, M. R. (1972-1973): Study on granitic plutons in the East Mongolia by gravity method. Institute of Earth Crust Academy of Science, Soviet Union - Mongolian Scientists Joint Geological Expedition, Academy of Science of USSR and Academy of Science of Mongolia, 72p. (in Russian).

4. No. 2447 Chirshov, L. D., Samovich, D. A. Markov, A. I. et al. (1976): Report on the result of aero- and auto-gamma spectrometric survey, scale 1:25,000 (geological survey MGSE-6) in the northeast Mongolian People's Republic in 1974-1975. Organization of Overseas Geology of Ministry of Geology, USSR and Mongolian Geological Survey Expedition, vol. I, 208p., vol. II, 282p. (in Russian).

5. No. 2416 Gusev, A. I., Chirshov, L. D., Tsaruk, I. I. et al. (1978): Report on the result of preliminary geological survey work on the scale of 1:50,000 in Ugtam volcano-tectonic depression area of North-Choibalsan district, MPR (geological survey MGSE-10) during 1976-1977. Organization of Overseas Geology of Ministry of Geology, USSR, and Mongolian Geological Survey Expedition, G. Irkutsuk, 218p. (in Russian).

6. No. 2459 Ministry of Geology, USSR, and Mongolian Geological Survey Expedition (1989): Geological structure and ore-prospective areas of North Choibalsan area of east Mongolia, Report on the result of search-evaluation and prospective work on geological survey MGSE-44 and theme 314 during 1986-1989. Dornod-Leningrad-Irkutsuk, vol. I, text 1, 95p., text 2, 296p., text 3, 95p. (in Russian)

7. No. 4441 Gombobaatar, O., Tsogtsaihan, B., Naranhuu, G., Chuluunsuh, S., (1990): Report on the results of geological mapping on the scale of 1:50,000 with general search in the Tsav-Bayan Uul ore zone during 1986-1990.
Ministry of Energy, Mining Industry and Geology MPR, Complexed Exploration *Geophysical Expedition, G. Ulan Bator, vol. I, 336p., vol. II, 83p. (in* Russian).

8. No. 4555 Mironov, U. B., Rubshov, G. V., Popov, V. G. (1990): Result of prospective geological survey and evaluation work in the North Choibalsan area, MPR. East Complexed Geological Expedition of Ministry of Geology, USSR, vol. I, text 1, 197p., vol., II text 2, 155p., vol. III, 29p., vol. IV, 123p., vol. V, text 1, 130p. (in Russian).

B. ULZIIT district

1. No. 578 Timofeeva, A. M., Chudinov, U. B. (1951): Geology and mineral resources of central part of Middle Govi Aimag, MPR. No. 130 Mapping Party of Sologoi Hudag, Huld Sum, 226p. (in Russian).

2. No. 4543 Narmandah, J., Enhbaatar, L., Erdenebileg, D., Hishigderger, D., Tuvsanaa, N., Hurelbuu, O. (1991); Report on the result of detailed prospecting work on the scale of 1:10,000 and mapping work of scale 1:50,000 inGurvan Saihan Area (1988-1991)., State Geological Center, MPR (in Mongolian).

Eaton, P. A. and Hohmann, G. W., 1989, A rapid inversion technique for transient electromagnetic sounding. Phys. Earth Planet Inter., vol. 53, p. 384-404.

Fullagar, P. K., 1989, Generation of conductivity-depth pseudo-sections from coincident loop and in-loop TEM data. Exploration Geophysics, p. 43-45.

Geonics Limited, 1992, GSPx7 & DATEM, PROTEM & EM37 Transient EM Software for PC/MS-DOS Compatibles.

Geonics Limited, 1992, PROTEM 57(C) OPERATING INSTRUCTIONS.

Interpex Limited, 1989, TEMIX USER'S MANUAL.

Nabighian, M. N. and Macnae, J. C., 1991, Time domain electromagnetic prospecting method, Chapter 6, vol. 2, in Electromagnetic Method in Applied Geophysics : Society of Exploration Geophysicists.

Oristaglio, M. L. and Hohmann, G., 1984, Diffusion of electromagnetic fields into a two-dimensional earth : A finite difference approach. Geophysics, vol. 49, p. 870-894.

Pellerin, L. and Hohmann, G., 1990, Transient electromagnetic inversion : A remedy for magnetotelluric static shifts. Geophysic, vol. 55, p. 1242-1250.

Raiche, A. P. and Gallagher, R. G., 1985, Apparent resistivity and diffusion velocity. Geophysics, vol. 50, p. 1628-1633.